Final deglaciation of the Malin Sea through meltwater release and calving events

Tarlati, S., Benetti, S., Callard, L., Ó Cofaigh, C., Dunlop, P., Georgiopoulou, A., Edwards, R., Van Landeghem, K. J. J., Saher, M., Chiverrell, R., Fabel, D., Moreton, S., Morgan, S., & Clark, C. D. (2020). Final deglaciation of the Malin Sea through meltwater release and calving events. *Scottish Journal of Geology*, *56*(2), 117-133. https://doi.org/10.1144/sjg2019-010

Published in:
Scottish Journal of Geology

Publication Status:
Published (in print/issue): 01/11/2020

DOI:
10.1144/sjg2019-010

Document Version
Author Accepted version

Sedimentological and microfaunal evidence for final deglaciation of the Malin Sea through meltwater release and calving events

Abbreviated title: Malin Sea shelf final deglaciation

Serena Tarlati*[1], S. Benetti[1], S.L. Callard[2], C. Ó Cofaigh[2], P. Dunlop[1], A. Georgiopoulou[3], R. Edwards[4], K.J.J. Van Landeghem[5], M. Saher[5], R. Chiverrell[6], D. Fabel[7], S. Moreton[8], S. Morgan[9], C.D. Clark[10]

[1] School of Geography and Environmental Sciences, Ulster University, Coleraine, UK
[2] Department of Geography, Durham University, UK
[3]UCD School of Earth Sciences, University College Dublin, Ireland
[4]School of Natural Sciences, Trinity College Dublin, Ireland
[5]School of Ocean Science, Bangor University, UK
[6]School of Environmental Sciences, University of Liverpool, UK
[7]Scottish Universities Environmental Research Centre, UK
[8]Natural Environment Research Council, Radiocarbon Facility, East Kilbride, UK
[9]University of Leicester, UK
[10]Department of Geography, University of Sheffield, UK
*Tarlati-S@ulster.ac.uk

Abstract *(199 words)*

During the last glacial maximum, the British-Irish Ice Sheet (BIIS) extended to the shelf edge in the Malin Sea between Ireland and Scotland, delivering sediments to the Donegal Barra Fan (DBF). The analysis of well-preserved, glacially-derived sediment in the DBF provides new insights on the character of the BIIS final deglaciation and on paleoenvironmental conditions at the Younger Dryas (YD). Chaotic/laminated muds, ice-rafted debris (IRD)-rich layers and laminated sand-mud couplets are interpreted as mass transport deposits, plumites and turbidites from BIIS-transported sediments. Peaks in IRD concentration constrained by radiocarbon dating to after 18 ka cal. BP indicate discrete

intervals of iceberg calving during the last stages of deglaciation. Glacially-derived sedimentation on the slope occurred until ~16.9 ka cal. BP. This is interpreted as the last time ice extended onto the shelf allowing glacial meltwater to reach the fan. Bioturbated and foraminifera-rich muds above glaciomarine sediments are interpreted as interglacial hemipelagites and contourites, with the presence of *Zoophycos* suggesting restoration of bottom currents at the transition between stadial and interstadial conditions. During the YD, *Neogloboquadrina pachyderma* sinistral abundances and an isolated peak in IRD indicate the temporary restoration of cold conditions and the presence of floating icebergs in the region.

Abstract *(199 words)*

During the last glacial maximum, the British-Irish Ice Sheet (BIIS) extended to the shelf edge in the Malin Sea between Ireland and Scotland, delivering sediments to the Donegal Barra Fan (DBF). The analysis of well-preserved, glacially-derived sediment in the DBF provides new insights on the character of the BIIS final deglaciation and on paleoenvironmental conditions at the Younger Dryas (YD). Chaotic/laminated muds, ice-rafted debris (IRD)-rich layers and laminated sand-mud couplets are interpreted as mass transport deposits, plumites and turbidites from BIIS-transported sediments. Peaks in IRD concentration constrained by radiocarbon dating to after 18 ka cal. BP indicate discrete intervals of iceberg calving during the last stages of deglaciation. Glacially-derived sedimentation on the slope occurred until ~16.9 ka cal. BP. This is interpreted as the last time ice extended onto the shelf allowing glacial meltwater to reach the fan. Bioturbated and foraminifera-rich muds above glaciomarine sediments are interpreted as interglacial hemipelagites and contourites, with the presence of *Zoophycos* suggesting restoration of bottom currents at the transition between stadial and interstadial conditions. During the YD, *Neogloboquadrina pachyderma* sinistral abundances and an isolated peak in IRD indicate the temporary restoration of cold conditions and the presence of floating icebergs in the region.

Keywords: deglaciation, marine terminating ice sheet, ice rafted debris, meltwater, plumites, Younger Dryas

The North Atlantic continental margin can be subdivided into three sedimentary settings: glaciated, glacially-influenced and non-glaciated margin in relation to the contribution of different depositional processes that produce distinct geomorphologies, including glaciogenic fans, complex canyon systems, areas of mass transport deposits and large contouritic drifts (Stoker 1995; Holmes et al.

1998; Weaver et al. 2000; Piper 2005; Sejrup et al. 2005; Stoker et al. 2005; Sacchetti et al. 2012a). North of 56°N, along the glaciated margin, glaciogenic fans, large sediment depocentres, built during glacial periods through downslope mass wasting, are the main sedimentary feature (Howe 1995; Armishaw et al. 1998; Howe et al. 1998; Weaver et al. 2000; Sejrup et al. 2005; Stoker et al. 2005). South of 56°N and north of 26°N, the continental slope was mostly shaped during glacial times by downslope sediment transport, mostly in the form of turbidity currents and mass wasting, resulting in intricate and dendritic canyon systems (Sejrup et al. 2005; Cronin et al. 2005; Ó Cofaigh et al. 2012; Sacchetti et al. 2012a). Along the western Irish and UK margin, the extension of the British-Irish Ice Sheet (BIIS) on the continental shelf contributed to the development of both glaciogenic fans and canyons north and south of 56°N. The Donegal-Barra Fan (DBF), located north-west of the island of Ireland (Fig. 1), was formed during Pleistocene glaciations and represents the southernmost of the North Atlantic glaciogenic fans, as well as the largest fan associated with the BIIS (Stoker 1995; Clark et al. 2012). As in similar settings along the Norwegian, Arctic, Antarctic and Canadian margins, the fan provides an ideal location for the investigation of the dynamics of marine-terminating ice sheets as it is more likely to contain a less disturbed and better preserved record of glacially-derived sediments compared to shallower water glacial deposits (Lucchi et al. 2015). Indeed, sediments on the DBF were previously studied to better understand the sedimentary evolution of the margin and the glacial history of the BIIS (Knutz et al. 2001; Wilson et al. 2002). Within this study, we investigated three sediment cores from the DBF, each between 6 and 7 m long, to reconstruct the deglaciation of the BIIS through the interpretation of sedimentary processes and relevant proxy records, namely Ice Rafted Debris (IRD) concentrations and foraminifera (*Neogloboquadrina pachyderma* sinistral) abundances. The aim of this paper is two-fold: 1) to describe and chronologically constrain the deglaciation of the BIIS using deep-water sediments and 2) to record the changing environmental conditions in this region from the last glacial to the present interglacial period.

Regional setting

The British-Irish Ice Sheet on the Malin Sea shelf

The BIIS was a largely marine-terminating and highly dynamic ice sheet that covered most of Ireland and Britain during its maximum extent (Scourse et al. 2009; Chiverrell & Thomas 2010; Clark et al. 2012; Peters et al. 2015; Callard et al. 2019). Several phases of advance and retreat on the continental shelf during the last glacial period have been inferred based on geomorphological and sedimentological evidence (Van Landeghem et al. 2009; Chiverrell & Thomas 2010; Dunlop et al. 2010; Clark et al. 2012; Ó Cofaigh et al. 2012; Peters et al. 2015; Callard et al. 2019). The BIIS reached its maximum extent on the outer Malin Sea shelf (MSs) at 27 ka, followed by a stepped retreat and possible periods of still-stand marked by grounding-zone wedges recently identified on the continental shelf, with smaller oscillations at millennial scale-variability identified in deep-water sediment records (Knutz et al. 2002; Wilson et al. 2002; Callard et al. 2019). These minor advances seem to correspond with the Dansgaard–Oeschger (D-O) multimillenial climatic cycles recorded in the Greenland ice cores and in the North Atlantic deep-water sediments (Wilson et al. 2002; Peck et al. 2006; Scourse et al. 2009). On the MSs, numerous glacial landforms (i.e. moraines, drumlins, iceberg scours and lineations) have been mapped and interpreted as related to the dynamism of the last BIIS (Benetti et al. 2010; Dunlop et al. 2010; Howe et al. 2012; Ó Cofaigh et al. 2012; Dove et al. 2015). These features suggest the presence of ice-streams flowing offshore from multiples directions from north-west Ireland and western Scotland (North Channel Ice Stream-NCIS, Hebrides Ice Stream-HIS in Fig. 1), before converging on the Malin Sea shelf and delivering large amounts of meltwater and sediment to the DBF. The HIS alone was calculated as draining between 5-10 % of the former BIIS (Dove et al. 2015). Glacial processes therefore transported glaciogenic sediment to the shelf edge and downslope to the DBF during periods of ice sheet maximum extent across the shelf (Knutz et al. 2001; Wilson et al. 2002; Bradwell et al. 2008; Dunlop at el. 2010; Dove et al. 2015; Ballantyne & Ó Cofaigh 2017; Small et al. 2017). The features also suggest episodes of BIIS advance and retreat and indicate that ice streaming occurred during ice sheet retreat and reorganisation within the last deglaciation (Dunlop et al., 2010; Dove et al., 2015). Scottish terrestrial evidence indicates that the total deglaciation of the BIIS marine termination along western Scotland and the Hebrides, with ice-streaming interruption and ice retreat to the coast line, occurred after 16 ka cal. BP (Small et al. 2016; Small et al. 2017). These previous reconstructions focussed on the deglaciation of the BIIS as recorded on the Malin Sea shelf, but the pattern of sedimentation along the slope and the DBF during deglaciation is still largely unexplored.

The Donegal-Barra Fan

From the end of the Pliocene, sedimentation along the NW European margin was driven by the Northern Hemisphere's extended glaciations that, through the extension of large marine-terminating ice sheets, shaped the shallow portions of continental margins and delivered sediments to the deep water (Stoker 1995; Davidson & Stoker 2002; Stoker et al. 2005; Sejrup et al. 2005; O' Reilly et al. 2007; Sacchetti et al. 2012a). On the Hebrides slope, the upper part of sedimentary sequence, which records the final seaward progradation of the continental margin through slope-front glaciogenic debris-flows, is referred to as the MacLeod sequence (Stoker et al. 1994; Stoker et al. 2005). The Donegal-Barra Fan (DBF), between 57° N and 55° N along the North East Atlantic margin, is part of this sequence and started forming during the Plio-Pleistocene (Fig. 1; Stoker 1995; Armishaw et al. 1998). The fan has often been described as the largest sedimentary body resulting from the drainage of the western BIIS, occupying an area of 6300 km^2 and with a maximum thickness between 400 and 700 m (Armishaw et al. 1998). It extends from the shelf edge at ca 200 m water depth to about 2000 m, to the north and south of the Hebrides Seamount and along the eastern flank of the Rockall Trough, which is a deep elongate basin orientated NE-SW parallel to the continental margin (Fig. 1; Ó Cofaigh et al. 2012; Sacchetti et al. 2012b). Many sediment lobes, extending up to 250 km in length, have been identified in recent studies and interpreted as the result of episodes of large-scale downslope mass wasting related to ice streaming across the Malin Sea shelf during glacial intervals (Knutz et al. 2002; Sacchetti et al. 2012a).

Regional oceanography

The main surface current in the North Atlantic is the North Atlantic Current (NAC). The NAC flows eastwards from the Gulf of Mexico across the Atlantic Ocean, then in an anticlockwise direction northward along the European coastline, before turning south as part of the sub-polar gyre. The Eastern North Atlantic Water (ENAW) originates from the NAC in the Bay of Biscay and is observed at ca. 1000-1500 m water depth on the eastern side of the Rockall Trough (Fig. 1 inset). It turns anticlockwise along the Hebrides Terrace Seamount and then moves south along the western margin of the trough (Holliday et al. 2000; Read 2000). It is advected northward by the Shelf Edge Current (SEC) with an average speed of 15-30 cm/s (New & Smythe-Wright 2001). In the deeper part of the basin and driven by the Deep Northern Boundary Current (DNBC), the North Atlantic Deep Water (NADW) flows along the lower continental slope and within the trough between 2 and 3 km water depth (Fig. 1 inset; McCartney 1992; Dickson & Kidd 1987). All of these currents are thought to be responsible for both the winnowing of sediments and the deposition of contourites on the continental margin in this region and the DBF (Faugeres et al. 1981; Howe 1996; Howe et al. 1998; Stoker 1997; Knutz et al. 2002; Masson et al. 2010; Georgiopoulou et al. 2012). During Quaternary glaciations, the release of large amounts of freshwater from ice sheets had a fundamental role on the deceleration or interruption of several Atlantic oceanic currents (Stanford et al. 2011; Bigg et al. 2012; Toucanne et al. 2015). The North Atlantic sediments recorded these oceanographic changes, as well as the restoration of typical interglacial oceanographic conditions following deglaciation (Rahmstorf 2002; McManus et al. 2004; Austin & Kroon 2001).

Materials and methods

The sediment cores analysed in this study were collected as part of the BRITICE-CHRONO project in 2014 by piston coring during cruise JC106 on the *RRS James Cook* (Table 1; Fig. 1). The cores were retrieved from the slope between water depths of 1036 m and 1537 m, with a recovery between 661 and 672 cm (Fig. 1; Table 1). Core sites targeted the DBF (Fig. 1) and individual sites were picked using acoustic data collected with a hull-mounted Kongsberg SBP120 sub-bottom profiler. This chirp system operates with a sweep frequency of 2.5 kHz to 6.5 kHz. The survey lines were collected perpendicularly to the margin, from the shelf edge to the base of the continental slope. In this study only one profile was used, it runs across the core location of JC106-134PC and JC106-133PC (Fig. 2). The data were imported into IHS Kingdom as 2D survey lines for visualisation and processing. The sub-bottom data are used in this paper to provide a broader stratigraphic context for the cores. Acoustic units were identified following the methodology outlined in Mitchum et al. (1977) and the depth and thickness in two-way travel time (twt-ms) of the units was converted using the average P-wave velocity acquired by multi sensor core logging of the recovered cores before splitting. The cores were analysed, soon after collection, with a Geotek Multi-Sensor Core Logger (MSCL) at 2 cm intervals for physical properties, then they were split, photographed and visually described. In this study specifically the magnetic susceptibility (MS) data are used as they best represent the variability of the lithofacies and their boundaries. X-radiographs were acquired at the School of Radiology at Ulster University, using a CARESTREAM DRX-Evolution System. X-radiographs were used to identify sedimentary structures not visible to the naked eye (cf. Howe 1995). Grain size analyses were carried out using a MALVERN Mastersizer 3000. Samples were collected ca. every 20 cm along core, soaked in a 50 ml 5% Calgon concentrated solution, then placed on a shaking table overnight to guarantee the disintegration of flocculated particles. The results are reported in mean volume weight values D(4;3) (cf. Mingard et al. 2009). X-radiographs, MS data and grain size distributions were used to aid lithofacies identification and interpretation.

Planktonic foraminifera and IRD counts were conducted in the fraction coarser than 150 µm, on 1 cm thick slabs collected at a 20 cm resolution down core and wet-washed at 63 µm. The counting included at least 300 specimens for the planktonic foraminifera and a minimum of 300 lithic grains, when recognised, for the IRD. IRD counts were carried out on a total of 106 samples across the 3 cores. IRD concentration [IRD] was calculated as the number of lithic grains on the total dry sediment weight (cf. Haapaniemi et al. 2010; Peck et al. 2006; Scourse et al. 2009). Calculation of the abundance for the polar species *Neogloboquadrina pachyderma* sinistral (NPS) was conducted with the aim of identifying colder stadial intervals. Foraminifera counts were conducted on 36 samples already collected for IRD counts and only in core JC106-133PC. This core was selected for the NPS analysis as it shows the most diverse sediment record of the three and is the furthest away from the former ice margin. Therefore, it is assumed that it represents a more open-water environment, likely to be affected by regional climatic and oceanographic changes, in addition to local and BIIS related proglacial processes.

A total of 7 AMS (Accelerator Mass Spectrometer) radiocarbon dates using monospecific planktonic foraminifera, or mixed benthic foraminifera were acquired for this study (Table 2). The samples typically targeted lithofacies boundaries or distinct peaks in the IRD content and were dated at the UK Natural Environment Research Council (NERC) Radiocarbon Facility (NRCF-East Kilbride) and the commercial analytical laboratory Beta Analytic. They were then calibrated using OxCal 4.2 (Ramsey 2009) with the Marine13.14c calibration curve (Reimer et al. 2013) which has an inbuilt 400-year marine reservoir correction. Table 2 presents the radiocarbon and calibrated dates, with three separate age simulations using ΔR values of 0, 300 and 700 years to account for uncertainty over the spatial and temporal variation in the marine reservoir effect ages in the North Atlantic and adjoining continental shelves since the Last Glacial Maximum (e.g. Wanamaker et al. 2012). For ease of presentation, only the calibrated ages with a ΔR of 0 years are used to describe the timing of events in the text. This protocol for reporting radiocarbon ages was agreed among the members of the BRITICE-CHRONO Consortium to allow for an easier comparison of results across the different transects. One sample was rejected from the age reconstruction because it was found to be collected in a disturbed interval, sample 133PC 375-376 cm. The radiocarbon dates were used for estimations of sedimentation rates, with the interpreted mass transport deposits and turbidites excluded from the calculations (cf. Benetti 2006). Furthermore, the correlation between the IRD and NPS records for the cores and the Greenland ice core isotope records helped, together with the radiocarbon dates, in time constraining the DBF sedimentary record (Peck et al. 2007; Haapaniemi et al. 2010).

Results

Acoustic data

<u>Description</u>

Four acoustic units are identified in the seismic profile. Acoustic unit 4 is recognised along the lower (1400-1600 m water depth, Fig. 2a), the middle (900 -1200 m, Fig. 2b) and the upper slope (above 900 m, Fig. 2c). It is characterised by sub-parallel, continuous, undisturbed reflectors of variable amplitude, with a wavy upper (purple in Fig. 2) boundary. It shows undulating sub-parallel and undisturbed reflectors in the lower slope (Fig.2a), with a thickness between 20 and 25 meters. It is between 30 and 45 m thick along the middle slope, with sub-parallel reflectors showing an asymmetrical aspect and up-slope propagation (Fig. 2b). In the upper slope, it is found deeper than 30 meters below sea floor (mbsf), with low amplitude and wavy, sub-parallel reflectors (Fig. 2c). No clear basal boundary is visible for the unit and the green highlighted reflectors (Fig. 2a,b) likely mark the lack of return for the seismic signal.

Acoustic unit 3 is recognised only along the upper slope overlaying unit 4. It has a varying thickness between 10 and 30 m, is bounded by continuous low amplitude reflectors (purple and light blue in Fig. 2c) and it shows an acoustically semi-transparent and chaotic character.

Acoustic unit 2 is present along the middle and upper slope, overlaying unit 4 on the middle slope and unit 3 on the upper slope. It ranges between 5 and 10 m of thickness (Fig. 2b,c) and it is internally characterised by low amplitude sub-parallel reflectors. Its upper boundary is represented by a high amplitude, undulated and discontinuous reflector (yellow in Fig. 2b,c). The lower boundary is the light blue low amplitude continuous reflector in the upper slope (Fig. 2c), and the high reflectance pink reflector along the middle slope (Fig. 2b).

Acoustic unit 1 is recognised overlaying unit 4 along the lower slope (Fig. 2a), unit 2 on the middle and lower slope (Fig. 2b,c). It is the uppermost facies observed, where it shows a thickness of approximately or lower than 3 m and is acoustically represented by low amplitude sub-parallel reflectors. Its upper boundary is the seabed, which is characterised by a high amplitude, undulated and continuous reflector (dark blue in Fig. 2a,b,c). JC106-133PC was recovered from the lower section of the slope and it sampled unit 1 and the top part of 4 (Fig. 2a). On the seabed, a ~6 m high escarpment is recognised at 1095 m water depth (middle slope). Core JC106-134PC was collected from this section of the slope (Fig. 2b) and it sampled seismic unit 1 and 2. Two escarpments (between 5 and 15 m high) are visible in the uppermost facies and at the seafloor along the upper slope (Fig. 2c), accounting for some of the discontinuity in the unit. No sediment cores were retrieved from this part of the slope.

A direct correlation between the acoustic units along the full length of the slope is not possible due to slope length and steep angle. Although, similar trends can be recognised through the singular slope sections, with no acoustic signal below 35 m, maximum thickness of the seismic units with largely high reflectance between 30 and 10 mbsf, and above these, seismic units thinner and with general low amplitude or transparency. Escarpments are predominantly found within these units.

Interpretation

The seismic line across the DBF shows a 2° steep (on average) slope marked by several escarpments (Fig. 2). Below ~35 m, due to lack of penetration, the record is interpreted as Plio-Pleistocene glaciogenic mass transport deposits based on previously published seismic and sedimentological/borehole records from the North Atlantic margin, which identify in the Upper

MacLeod sequence, a stack (up to 60 m thick) of reworked glaciomarine sediments (Stoker et al. 1994; Stoker 1995).

Acoustic unit 4, together with unit 2, which are of similar character, are interpreted as consisting of Late Pleistocene glaciomarine sediments, also part of the Upper MacLeod sequence. In the lower and middle slope, (Fig. 2a and 2b), these units show continuous and subparallel reflector. Additionally, in the middle slope, the unit displays upslope-climbing sediment waves (Fig. 2b). This configuration is typical of sedimentary wave migration during intervals of large sedimentary input and high sedimentation rates, which could be related to downslope and along slope sediment transport (Wynn & Stow 2002). The upper acoustic unit of the Upper MacLeod sequence was also characterised by continuous, wavy and subparallel reflectors and it was interpreted as distal glaciomarine sediments redistributed by different mass flow processes as mass wasting and turbidites along the Hebrides slope and the Barra Fan (Stoker et al. 1994; Stoker 1995; Armishaw et al. 1998; Knutz et al. 2002).

The character of the upper slope observed in acoustic unit 3 (Fig. 2c) is slightly different (i.e. chaotic and semi-transparent). A similar acoustic facies, interpreted as debrites, is found on the Donegal Barra Fan in correspondence of the Peach Slide (Owen et al., 2018). The occurrence of the buried escarpments specifically within unit 2 seems also to suggest that the upper slope was likely affected by down-slope mass movements and slumps.

The uppermost acoustic unit 1, along the entire slope, is interpreted as recording Holocene hemipelagic and contouritic deposition as observed elsewhere on the fan, where similar acoustic facies and sediments are identified and dated (Armishaw et al. 1998; Knutz et al. 2002; Owen et al. 2018). The reduced thickness compared to the underlying units (~3m vs. 30-40m) suggests a reduced sediment input compared to the previous conditions during the Late Pleistocene.

Chrono- and lithostratigraphy

<u>*Lithofacies description*</u>

Five lithofacies are defined based on lithology, sediment colour, internal sedimentary structures observed in the X-radiographs, mean grain size (volume weight mean D (4,3)) and magnetic susceptibility (Fig. 3-7).

Laminated mud rich in IRD (ILM): This lithofacies is an olive-brown laminated mud rich in ice-rafted debris (IRD). The diameter of the IRD grains, observed on the split sediment core and by the x-radiographs, ranges from a few mm to 5-6 cm in diameter and the grains are not equally distributed within the facies. Laminations are not always visible to the naked eye but clearly evident on the X-radiographs (Fig. 3). Bioturbation is not noticeably present and foraminiferal content is low. The mean volume grain size is extremely variable due to the IRD content, fluctuating from 10 to 100 µm. Magnetic susceptibility ranges between 80 and 150 (10^{-5} SI) (Fig 4-6). This laminated IRD-rich mud is found in all three piston cores, constitutes the majority of the sediment record and has a thickness of up to 3.5 m (Figs 4, 5 and 6).

Chaotic mud (CM): This lithofacies is an olive-brown, chaotic mud, poorly sorted, devoid of foraminifera, with well-defined shear surfaces and occasional mud clasts (Fig. 3). No primary sedimentary structures are present but rare wispy and dipping laminations are observed (Fig. 3). It is present in all the cores and shows a thickness varying from 20 cm to ca. 50 cm (Figs 4, 5 and 6). The grain size is measured as < 20 µm in volume weight D(4;3).

Laminated sand to mud couplet (LSM): Olive-brown laminated sand to mud couplets, with laminated basal sand and sharp basal contacts are observed in all cores. This lithofacies has a fining upward trend with a coarser sand base gradually fining into mud within the unit (Fig. 3). Ripples are recognised within the sandy interval, bioturbation is absent and foraminifera are scarce. Generally, the couplets are between 5 cm to 10 cm thick and the facies is marked by high magnetic susceptibility, with values between 160 and 270 (10^{-5} SI) (Figs 4, 5 and 6).

Extensively bioturbated mud (BM): This lithofacies is a brown mottled sandy mud, rich in foraminifera and extensively bioturbated (Fig. 3), showing an abundant presence of *Zoophycos* burrows. *Zoophycos* is an ichnofacies, characterised by long tubular structures parallel and sub-horizontal within the sediment, with a thickness not less than 1 cm (cf. Löwemark et al. 2006). The distribution of this ichnofacies in the JC106 cores varies with core depth. The burrows are abundant at the base of this facies but reduce in number moving upwards in the sediment record. This facies is found in all of the three piston-cores collected from the DBF: at the core top of JC106-133PC and JC106-134PC, and below the foraminifera-bearing mud lithofacies in core JC106-128PC (Figs 4, 5 and 6). It is up to 2 m thick and generally darker than the sedimentary unit above (FM) and lighter in colour from the facies below (ILM). Within this lithofacies both fining and coarsening upward trends in grain size were observed during the visual core descriptions and in the x-radiographs, with both sharp and gradual basal and upper contacts. This facies has a high content of foraminifera and the characteristic grain size is calculated between 20 and 40 µm in mean volume weight D(4;3). Magnetic susceptibility varies greatly within the facies and it is between 40-120 (10^{-5} SI) (Figs 4, 5 and 6). No primary sedimentary structures are visible.

Foraminifera-bearing mud (FM): A light brown, sandy foraminiferal mud was recognised only at the top of core JC106-128PC. This facies shows bioturbation, clearly visible in the X-radiographs (Fig. 3). The mean volume grain size is 30-40 µm, with the foraminifera representing the coarser fraction. It has a thickness of approximately 5 cm and there is a gradual contact with the darker underlying lithofacies (BM). The acquisition of physical properties was not possible in this facies because of its limited thickness and position at the core top.

<u>*Lithostratigraphy*</u>

Core JC106-133PC, the deepest and most westerly located core (Figs 1 and 4), contains laminated IRD-rich mud (ILM) from the base at 660 cm bsf up to 370 cm down core. Three intervals of laminated sand to mud couplets (LSM), with thicknesses varying between a few cm to 7-8 cm, were identified around 380 cm, 390 cm and 444 cm down core, highlighted by increased MS values, reaching over 200 (10^{-5} SI). ILM change gradually over 10 cm into extensively bioturbated mud (BM), which extends up to 185 cm core depth. Within BM, a chaotic mud (CM) interval was recognised at 275 cm, with a 7 cm thickness. Above 185 cm down core, the laminated IRD-rich mud facies is again present and has a thickness of ca. 50 cm, followed by a gradual upper contact over 5 cm into another BM interval that continues to the core top.

In core JC106-128PC (Figs 1 and 5), IRD-rich laminated mud (ILM) is the dominant lithofacies from the core base to 95 cm core depth. Four chaotic mud (CM) deposits, bounded by inclined and sharp planes, are identified through the ILM interval at 310 cm, 449 cm, 547 cm and 590 cm down core, with thickness ranging between 5 and 25 cm. A LSM interval at 182 cm core depth displays a sharp basal contact and a thickness of 8 cm and it is well visible by a peak in MS reaching 160 (10^{-5} SI). Above 95 cm, ILM gradually passes into BM over a few cm. This extensively bioturbated mud extends up to 5 cm down core, interrupted by a 5 cm thick laminated mud at 30-35 cm with sharp basal and gradual top contact. There is a gradual transition from BM to foraminifera-bearing mud (FM), visible between 5 cm and the core top. The FM lithofacies is found exclusively at the core top of 128PC (Figs 1 and 5).

In core JC106-134PC, the more proximal to the shelf edge (Fig. 1), ILM represents the main lithofacies, extending from the base of the core up to 120 cm down-core. At 444 cm down-core a sharp increase is seen in the magnetic susceptibility signal (Fig. 6), with a high value of 346 (10^{-5} SI) which correspond to large lithic grains, easily recognised at the x-rays. A 1m-thick chaotic mud deposit is recognised between 210 cm and 310 cm, with an inclined sharp surface at the top and faint and inclined lamination within it. A laminated sand to mud couplet (LSM) is observed at 198-195 cm, it is indicated by an increase in the mean volume grain size and a peak in MS of 200 (10^{-5} SI).

Above ILM, BM extends with a gradual contact from 120 cm core depth up to the core top. A 10 cm-thick CM deposit was recognised at 50 cm bsf. This unit is wedge shaped and marked by two inclined (up to 45°) sharp surfaces, bounded with fine silt (Fig. 3).

Overall, the three cores show a similar alternation of lithofacies from base to top and result in a similar internal organisation (Figs 4, 5 and 6), although core JC106-128PC differs in that it contains a larger number of chaotic mud deposits compared with the other two. Generally, the IRD-rich laminated mud constitutes the majority of the sediments and the facies is recognised in the lower half of the sediment record in the cores. Within the top of ILM, during the transition to BM, the laminated sand to mud couplets (LSM) are identified in all the three cores. The LSM are always recognised in the upper part of the ILM. Conversely, the CM lithofacies does not display a noticeable trend as these intervals are present through the record. BM is characteristic of the upper part of JC106-133PC and JC106-134PC, but not of JC106-128PC. A thin (5 cm) interval of foraminiferal-bearing mud (FM) is recognised at the top of JC106-128PC (Fig. 5). This facies does not seem to be present in the other two sediment cores. An IRD-rich mud interval is identified through the BM facies in JC106-133PC and JC106-128PC, with a thickness of 45 cm at 1537 m water depth and 5 cm at 1475 m water depth, but it is not recognised in JC106-134PC, the shallowest of the cores. The interval is highlighted by high values of MS, ranging between 160 and 200 (10^{-5} SI) (Figs 4 and 5).

Radiocarbon dating and sedimentation rates

Radiocarbon ages constrain most of the sediment record to the end of the last glacial interval (Marine Isotopic Stage 2 - MIS2). In the cores the oldest age of 17,825 ± 175 cal. BP is found between 583 and 588 cm down core in JC106-133PC, within the ILM lithofacies. The youngest age is observed in the same ILM lithofacies, at 175 cm in the same core, corresponding to 12,690 ± 90 cal. BP. The available ages constrain the boundary between the laminated mud rich in IRD and the extensively bioturbated mud ranging from 16 to 15.2 ka cal. BP.

The sedimentation rates calculated for the laminated mud rich in IRD are 166 cm/ka for JC106-134PC (closest to the continental shelf break), and 131.8 cm/ka for JC106-133PC (furthest from the shelf break). Rates for the extensively bioturbated mud (BM) facies show much lower values, ranging from 3.7 cm/ka for JC106-134PC to 21 for JC106-133PC.

<u>Ice-rafted debris (IRD) concentration and Neogloboquadrina pachyderma abundance</u>

IRD is mainly represented by crystalline quartzite, granite and basalt. These petrologies were previously recognised as typical of the Irish and Scottish geology (Knutz et al. 2001) and therefore likely to be related to the delivery of IRD by the BIIS during its advance and retreat in the Late Quaternary. IRD is found within the laminated mud lithofacies at an average concentration of 960 grains/g of dry sediment in JC106-133PC, 1150 grains/g in JC106-128PC and 1350 grains/g in JC106-134PC (Figs 4, 5 and 6). The lowest [IRD] values are generally measured at the core tops and within the BM lithofacies. The highest concentrations are observed in lithofacies ILM, 6730 grains/g of dry sediment, at 350 cm down-core in JC106-134PC (the most proximal core to the shelf edge; Fig. 6).

In core JC106-133PC, [IRD] is very low within the BM lithofacies, with values close to 0 (Fig. 4). In the ILM, the [IRD] increases to a minimum of 1000 grains/g. Three main IRD peaks are observed at 175 cm, 453 cm and 585 cm with respective values of 1420, 2340 and 3600 grains/g. These peaks are relatively sharp and represent a two- to three-fold increase in IRD concentration compared to the values above and below them. Core JC106-133PC shows consistently high [IRD] in the bottom half (Fig. 4), on average 1656 grains/g per sample. Within the upper part of the core, an interval with a peak [IRD] is recognised between 140 and 175 cm, with values up to 1428 grains/g. In core JC106-128PC, the [IRD] shows an irregular pattern, displaying many peaks with maximum values of 2180 and 1910 grains/g (Fig. 5). The lowest values (<200 grains/g) are measured in the BM lithofacies; while in the ILM, peaks are observed with values of 1030 and 1620 grains/g. The highest peaks are recognised within chaotic muds. In core JC106-134PC, the lowest [IRD] are measured through the

BM lithofacies with values between 0 and 1000 grains/g (Fig. 6). A general increase is observed in the ILM lithofacies, with an average of 1547 grains/g per sample. As previously observed in JC106-128PC, the increase in [IRD] can sometimes be correlated to the presence of chaotic mud deposits along core. Two [IRD] peaks within the ILM are recognised at 350 and 550 cm with values of 6730 and 3026 grains /g.

The abundance of the planktonic foraminifera *Neogloboquadrina pachyderma* sinistral (NPS%) calculated in core JC106-133PC shows an alternation between high and low values (Fig. 4). The NPS% abundance mirrors the IRD curve, with high NPS% corresponding with IRD peaks and characterising the ILM lithofacies. NPS% is low at the core top, with values <10% of the planktonic foraminifera assemblage between the core top and 120 cm of core depth. Further down the core, a sudden increase between 140 and 195 cm is recorded with NPS% >=80%. Between 195 cm and 355 cm down-core, the NPS% is reduced again to values <10 %. At 375 cm of core depth, the NPS abundance increases suddenly and significantly, exceeding values of 80%, and remains high in the lower part of the core to the base.

Discussion

Chronostratigraphy

The chronostratigraphic framework for the sediment cores is reconstructed using the radiocarbon dates together with *Neogloboquadrina pachyderma* sinistral abundance (NPS%) and the IRD record. NPS% commonly indicates changes in sea-surface temperature and it is known to represent the most abundant polar species during cold intervals in this region (Bond et al. 1993). In this region, NPS% has been previously observed having a direct correlation with BIIS-delivered IRD and air temperature changes recorded in ice masses, making it possible to correlate it with the GISP2 ice-record from Greenland (Peck et al. 2006; Peck et al. 2007; Haapaniemi et al. 2010). In core JC106-133PC, the NPS% also shows a direct correlation with the IRD concentration (Fig. 4). Therefore, the trends in [IRD] in all cores were tentatively correlated with the oxygen isotopic record from the GISP2 ice-record from Greenland (Rasmussen et al. 2014). This was done in order to establish the chronostratigraphy of the sediment record, to identify possible stadial and interstadial periods and to allow comparison with the previous works in this area (Fig. 7). Based on the available radiocarbon dates and the pattern of IRD distribution, the entire sediment record appears to be younger than 18 ka cal. BP and therefore time-constrained to Marine Isotopic Stage (MIS) 1 and the latter part of MIS2 (Figs 7 and 8). Based on the correlation between the DBF IRD record and the GISP2, together with the acquired radiocarbon dates, the laminated mud rich in IRD (ILM), characterised by high NPS abundance and IRD concentrations, is thus dated to the Greenland Stadial 2 (GS-2) (23 to 14.7 ka cal. BP). The ensuing extensively bioturbated muds (BM) were likely deposited during the Bølling-Allerød interstadial (14.7-12.8 ka cal. BP) or Greenland interstadial 1 (GI-1). ILM is again identified within the YD or Greenland stadial 1 (12.9 to 11.5 ka cal. BP), in core JC106-133PC. After the YD, a return to BM deposition follows during the Holocene. The reduced thickness of the BM in cores JC106-128PC and JC106-134PC is interpreted as representing a low sedimentation rate following the GS-2 (hypothetical values indicated in Fig. 7) or a possible hiatus in sedimentation as no clear YD IRD record is evident in the two cores (Fig. 8).

Based on acoustic units thicknesses, unit 4, 2 and 1 (Fig. 2) contain all the lithofacies observed in the cores and these are therefore interpreted as representing sedimentation post last glacial maximum (LGM).

Sedimentary facies interpretation

The five lithofacies identified in the sediment record are interpreted as corresponding to five different sedimentary processes, all characteristic of sedimentation along a glaciated margin (Fig. 8; Hesse et al. 1997; Weaver et al. 2000; Ó Cofaigh & Dowdeswell 2001; Lucchi et al. 2002). All the core bottoms show deposition of laminated mud rich in IRD (ILM) on the DBF between ~ 18 ka cal. and 16 ka cal. BP. Based on the planar laminations, relatively high sedimentation rates, presence of IRD and lack of bioturbation, the ILM facies is interpreted as a plumite. The facies is read as being deposited mostly by settling of fine-grained sediments from meltwater plumes, in conjunction with ice-rafted material from icebergs (cf. Wang & Hesse 1996; Hesse et al. 1997; Dowdeswell et al. 1998; Hesse et al. 1999; Ó Cofaigh & Dowdeswell 2001; Evans et al. 2002; Lekens et al. 2005; Lucchi et al. 2002; Roger et al. 2013; Prothro et al. 2018). Meltwater plumes have been observed to deliver fine sediment up to 250 km from the basal ice sheet meltout location (Hesse et al. 1997; Prothro et al. 2018) and in this study the cores are retrieved at a maximum of 200 km from the inferred closest ice-margin. The BIIS former ice margin was in fact located at this time on the Malin Sea Shelf, along Western Scotland and the Hebrides (Finlayson et al. 2014; Small et al. 2017; Callard et al. 2019). Within the facies, the main IRD petrologies include basalts, quartzite and highly metamorphic rocks, and they do not show any significant variation in abundance/composition along core. The highest IRD concentrations are inferred to be related to a relative enrichment of icebergs due to calving events (cf. Andrews 2000; Scourse et al. 2009).

The laminated sand to mud couplets (LSM) found within the plumites with the fining upward grain size and the sedimentary structures, such as ripples and planar lamination, suggest that they are deposits of dilute, low-density turbidity currents (Middleton & Hampton 1976; Lowe 1979; Lowe 1982; Wang & Hesse 1996; Hesse et al. 1997; Hesse et al. 1999). Based on the core chronostratigraphy, they likely deposited around 17 ka cal. BP and their occurrence is inferred as related to the meltwater release (Fig. 8). The identification of turbulent flow deposits along the margin also suggests the deposition of sediment from glacial meltwater during the final stages of BIIS melting, with consequent slope instability during deglaciation. Hyperpycnal flows and the direct flow of fresh sediment-laden waters into the ocean, are indeed identified as one of the possible mechanisms for the generation of turbidity currents and they have been described from modern tidewater glaciers and inferred from sediment records from other formerly glaciated margins (Piper and Normark 2009). A similar behaviour along polar and north Atlantic margins is recorded in a rhythmic turbiditic activity, used as a proxy for meltwater delivery during the last deglaciation (Dowdeswell et al. 1998; Roger et al. 2013).

Overlying the plumites, the extensively bioturbated mud facies (BM) is interpreted on the basis of lack of primary sedimentary structures, bioturbation, mottling and low sedimentation rates (Figs 7 and 8) as contourites (i.e. sediment reworked and winnowed by bottom-currents; Stow 1979; Stow & Lovell 1979; Stow & Piper 1984; Stow et al. 2002; Rebesco et al. 2014). The transition from plumite to contouritic deposition occurred between ~16 and ~15.2 ka cal. BP and seems to continue to modern day (Fig. 8). Based on their mean grain size (<30 μm), the contouritic deposits can be classified as muddy contourites (cf. Stow et al. 2002; Rebesco et al. 2014). The *Zoophycos* ichnofacies within the contourites allows for the identification of an initial restoration of the bottom currents and of intermediate climatic conditions in the region at this time. This *ichnofacies* appears to be dominant and is consistent with a well-developed burrowing network in deep-water ecosystems that developed at the transition between cold and warm climatic stages (Dorador et al. 2016). The top of the contourites has not been dated, but the facies is recognised to the tops of cores JC106-133PC and JC106-134PC (Fig. 8). In cores JC106-134PC and JC106-128PC, the BM unit is between 120 and 95 cm thick, which seems to suggest a very condensed post-deglaciation and Holocene sediment record, or the presence of a sedimentary hiatus. If the core top represents modern day sedimentation, the average sedimentation rate since ~ 15 ka cal. BP would be ca. 3.5 cm/ka for JC106-134PC and < 7.8 cm/ka for JC106-128PC. Conversely, in core JC106-133PC, the contouritic unit is 360 cm thick but it is interrupted by a 50-cm thick plumite interval (Fig. 4). This corresponds to an average sedimentation rate of 21 cm/ka for the same period. The contouritic unit is interpreted as being initially deposited during the transition between stadial and interstadial conditions, with relative high sedimentation rate (between 20 and 5 cm/ka) and presence of *Zoophycos* as observed elsewhere along the Atlantic margin (cf. Dorador et al. 2016).

Chaotic muds (CM) occur within the plumite and the contouritic facies (Fig. 8). Chaotic muds are interpreted as mass transport deposits due to slope instability (Holmes et al. 1998; Tripsanas & Piper 2008). The interpretation is supported by the identification of inclined (up to 45°; Fig. 3) sharp contacts inferred as shear surfaces and the presence of mud clasts. Similar deposits have been identified within glaciogenic sediments along other glaciated margins (Aksu & Hiscott 1989; Tripsanas & Piper 2008; Garcia et al. 2011).

The thin (5 cm) interval of foraminiferal-bearing mud (FM) at the top of JC106-128PC (highlighted in Fig. 8 by the yellow arrow) is interpreted as a hemipelagite. It is the result of slow settling of fine mud and foraminiferal tests, where bioturbation is common and the depositional environment is characterised by low energy (Stow et al. 1996; Stow & Mayall 2000; Howe 1995; Knutz et al. 2001). The hemipelagite is not directly dated but its similarities with other deposits reported in the vicinity, such as characteristic colour, presence of foraminifera and the core top position (along the Irish margin: Howe1995; Knutz et al., 2002; on the DBF: Howe 1996; Knutz et al. 2001; Wilson et al. 2002; and in the Rockall Trough: Howe 1995; Georgiopoulou et al. 2012) suggest that this facies represents the most recent Holocene deposition. The hemipelagite does not seem to be present in JC106-133PC and JC106-134PC; its absence could be attributed to the presence of erosional bottom currents at specific water depths in the region, but also to coring disturbance, as it is likely to lose the top few centimetres of sediment record when piston coring (Buckley et al. 1994).

The Late Quaternary DBF sedimentary record

The interpretation of the sedimentary processes and their timing, derived from the radiocarbon dates and the correlation between the IRD and the GISP2 oxygen isotope records, reveal how sedimentation in the DBF evolved during the Late Quaternary as the BIIS margin retreated from the shelf edge (Fig. 9). Within the studied DBF record, the plumites calculated sedimentation rates ranges between 160 and 130 cm/ka, with the lower values in core JC106-133PC, the most distal from the shelf edge. The high sedimentation rates in the plumites suggest that these have been delivered through concentrated meltwater plumes and icebergs, confirming the presence of a melting and retreating BIIS along western Scotland and the Hebrides. The DBF glaciomarine sediments were delivered by meltwater plumes during the last period of BIIS marine extension, representing the deglacial sedimentary record of the retreating Hebrides Ice Stream (HIS). The HIS provenance is suggested given the close proximity of the DBF to the Outer Hebrides (approximately 100 km), with a less likely North Channel Ice Stream contribution, merely based on relative distance from the ice margin. The total deglaciation of the MSs, with retreat of the ice-limit to the present coast line and consequent interruption of the HIS, has been dated between 17-16 ka cal. BP (Bradwell et al. 2008; Small et al. 2017; Ballantyne & Ó Cofaigh 2017; Callard et al. 2019). Other evidence along western Scotland suggests that the BIIS was extending onto the MSs until around ~16 ka cal. BP (Dove et al. 2015; Small et al. 2016; Small et al. 2017). These previous works in the area support the possibility of a large deglacial record deposited in the deep water and allow to confirm that the sedimentary evolution of the fan was largely related to the BIIS extension up until its final retreat onshore.

Following deglaciation, the continental slope of the DBF experienced a progressive strengthen of bottom currents. The *Zoophycos* ichnofacies is visible in the contourite deposited just after the BIIS deglaciation and the YD, it suggests an increase in temperature and a restoration in ocean currents speed following the current weakening during the cold stadials. The decrease in *Zoophycos* burrows toward the core top in BM is attributed to an increasing bottom current velocity and temperature through time, representing a transition to modern climatic conditions. Such an increase in current speed would have had the potential to winnow the sediments in the study area and may be responsible for the limited thickness of the post-glacial and Holocene sediments. The thickness of the contourites appears to increase with water depth and this is proposed to be linked with variations in bottom current speed, with higher speed along the shallower section and lower speed at depth, with a reduced erosive power or possible settling of material. Hiatuses in the DBF record were observed in previous studies and attributed to the NADW current, which could winnow or hinder hemipelagic deposition during the Late Pleistocene and Holocene on the North East Atlantic continental slope (Knutz et al. 2002). The sediment record from the JC cores confirms these previous observations from elsewhere on the DBF and suggests that the winnowing of Holocene sediments is active between 1000 m and 1500 m of water depth, in correspondence of the flow of ENAW.

Hemipelagite deposition is not particularly prominent along this stretch of the margin and only a thin hemipelagic layer is present at the top of core JC106-128PC. We can only speculate that this hemipelagite represents the most recent sedimentation and that the transition into this different style of sedimentation could be related to further changes in oceanic circulation and/or reduced sediment supply in the study area. However, our data is too limited to discuss this any further.

IRD peaks and calving events

Three peaks in IRD are identified and interpreted as an increased release of IRD due to iceberg calving events. Iceberg calving is suggested as the mostly likely process for the delivery of sand and coarse size lithic grains to the core sites (Lekens et al. 2005; Rorvik et al. 2010). These peaks are tentatively correlated across the cores and the two main events are dated before 16 ka cal. BP: one was directly dated at ~17.8 ka cal. BP, whilst the younger is inferred to have been deposited around ~16.9 ka cal. BP based on the calculated sedimentation rate on JC106-133PC (blue arrows in Fig. 7). The third IRD peak, only recognized in core JC106-133PC, the most distal from the MSs, is directly dated at ~ 12.7 ka cal. BP (i.e. during the Younger Dryas; Alley 2000).

During MIS 2, the peaks are interpreted as the result of BIIS calving events, in particular from the HIS section of the ice sheet as it retreated towards land at this time. For the YD plumite characterised by a high [IRD] and NPS% a different origin for the icebergs is suggested. Previous studies on sediment cores from the North East Atlantic margin showed a similar enrichment in IRD during YD that was attributed largely to the Laurentide Ice Sheet, with the potential presence of a calving ice sheet in Scotland (Scourse et al. 2009). Recent evidence indicated that the Scandinavian Ice Sheet (SIS) extended offshore south-west of Norway during the YD (Broecker et al. 2010; Mangerud et al. 2016). Additional evidence suggests that the main oceanic currents weakened, similarly to what happened during the previous glacial period (Austin & Kroon 2001; Peck et al. 2006; Adams et al. 1999; Broecker et al. 2010; Lynch-Stieglitz et al. 2011). Based on previous reconstructions of ice-sheets history along the NE Atlantic margin, in particular during the YD (Hughes et al. 2015;

Mangerud et al. 2016), we postulate that the YD DBF received a high IRD discharge likely related to a SIS advance and an associated icebergs flowing south along the Atlantic margin. A SIS origin is suggested considering that the IRD petrographies in the YD-dated interval are represented largely by quarzite, basalt and highly metamorphic grains, corresponding with a European origin/geology (http://www.ngu.no/emne/regionalgeologi). These petrologies are typically found along the Scandinavian margin as well as the southern located UK and Irish margin, and they represent the majority of the lithics identified in this study. The IRD petrologies, together with a non-previous recognized BIIS marine extension able to deliver meltwater plume and iceberg to the fan during the YD, is interpreted as potentially related to icebergs from the documented extended SIS. A detailed investigation of the IRD record, with calculations of relative abundance of the IRD petrologies was not part of the project and is strongly suggested for future studies as it may provide clear evidence for icebergs provenance.

Comparison with other glaciated margins

Most of the JC106 sediment record from the DBF is interpreted as representing the sedimentation occurring during the final stages of the last BIIS deglaciation, at the end of the Late Midlandian glaciation (MIS2). Between ~18 and ~16 ka cal. BP, the DBF received meltwater and IRD from the BIIS before complete ice-depletion. This suggests that meltwater and iceberg discharge during the latter part of the deglaciation significantly contribute to the build-up of the DBF, in addition to the downslope sediment transport observed occurring during the broader last glacial interval (Howe 1995; Stoker 1995; Armishaw et al. 1998; Holmes et al. 1998; Sejrup et al. 2005).

The DBF deglacial sediment record analysed in this study shows similarities with most records of other glaciated margins and glaciogenic fans. These similarities are recognised in the style of sediment deposition, in particular the presence of plumites, recognised along the Northern North Sea, the Norwegian Margin, the Barents Sea and the Canadian Slope (Hesse et al. 1999; Lekens et al. 2006; Lucchi et al. 2015). The sedimentation rates calculated for the plumites on the Norwegian margin vary between 20 and 2000 cm/ka (Lekens et al. 2005; Hjelstuen et al. 2009). In addition, along the Southern Norwegian Margin the ice stream activity also is recognised concluding through calving events, recorded as high content of IRD within the plumites (Lekens et al. 2005).

Our data show that the deep water environment and the slope are still largely influenced by the BIIS activities during the final moment of ice sheet extension offshore. The meters-thick plumite intervals on the DBF show how the marine terminating ice sheets are still able to deliver sediments with relatively high sedimentation rates through meltwater plumes, up to the ice sheet retreat onshore. The delivery of glaciogenic sediment to the fan during deglaciation, once the ice sheet retreated from the shelf edge, is inferred to have occurred largely by meltwater processes and iceberg rafting. The latter is based on the presence of IRD peaks within the plumites. This contrasts with periods when the ice sheet was positioned at the shelf break during glacial maxima and glaciogenic sediment delivery to the fan was dominated by downslope mass transport, particularly by gravity flow processes (cf. Dowdeswell et al. 1998).

More widely this highlights differences in the nature of sediment delivery on glaciated continental margins such that high-latitude slopes, along the Norwegian and Svalbard margins (e.g., Dahlgren & Vorren 2003; Jessen et al. 2010), are dominated by downslope sediment transport, especially that related to glaciogenic debris flows (Laberg et al. 2000); whereas, further south along the Irish margin and on the DBF the contribution of meltwater delivery becomes much more significant. The latter is consistent with studies from the Canadian margin, in particular the Scotian slope (e.g., Piper 1988) where meltwater delivery was a major contributor to margin development particularly during deglaciation of the Laurentide Ice Sheet (LIS). The ice loss from the southern portion of the LIS occurred mostly by melting due to the thermal gradient along the margin (Piper 1988); such a gradient could similarly be the cause of the varying style of ice loss along the NE Atlantic discussed here.

Implication for climate reconstruction in the North Atlantic

BIIS calving events have previously been interpreted as independently regulated by the internal ice-sheet dynamics on a millennial (D-O) time scale (Knutz et al. 2001; Wilson et al. 2002; Peck et al. 2006; Haapaniemi et al. 2010). From a broad perspective, a synchronicity in the final deglaciation of European Ice Sheets (EIS), including the BIIS, the Scandinavian Ice Sheet, the Svalbard-Barents-Kara Seas and the Channel River Hydrographic Network, along the North East Atlantic was suggested (Hughes et al. 2015).

The EIS, which similarly to the Laurentide Ice Sheet delivered large amounts of freshwater to the North Atlantic Ocean, is considered responsible for global climatic changes during the deglaciation (Bigg et al. 2012; Toucanne et al. 2015). The BIIS dynamics, together with the other European Ice Sheets, can therefore be considered as having an active and contributing role on the North Atlantic climate. The reconstructed dynamic behaviour of the BIIS from the DBF sediment record seems to show some synchronicity with the ice margin further south. In particular, sediment retrieved from the Bay of Biscay showed two large discharges of meltwater from the EIS occurring at 18.2 ± 0.2 and 16.7 ± 0.2 ka cal. BP (Toucanne et al. 2015). These timings are very similar to those of the IRD peaks recorded in the DBF and inferred as large release of meltwater and calving events during the deglaciation of the Malin Sea shelf and the Hebrides Ice Stream. Additionally, both the DBF and Bay of Biscay records show glacial instability and ice wasting during stadial Heinrich stadial 1 (HS1) (18.2-16.7 ka BP), which represents the time period when the Laurentide Ice Sheet (LIS) instability reached its maximum, including the occurrence of Heinrich 1 event (Heinrich 1988). The synchronicity in the deglacial meltwater release between the BIIS and the EIS, and further afield with the LIS, highlights a potential climatic relationship among the circum-North Atlantic ice-sheets, at least in their final deglaciation. Given the potential effect of the release of large amount of meltwater on the North Atlantic circulation, it is possible that these pulses in deglaciation may explain some of the observed variability in the North Atlantic Ocean circulation at this time (cf. Bigg et al. 2012).

Conclusions

The investigation of the deep water sediments retrieved from the DBF allowed for the reconstruction of the final stages of the BIIS deglaciation, since 18 ka cal. BP, and the transition to modern climatic conditions (Fig. 9).

- The DBF sedimentary history from the last ~ 18,000 years was reconstructed. The sediments record deposition from meltwater plumes with high sedimentation rates during the final BIIS deglaciation, with a post-glacial restoration of oceanic currents and deposition of contourites during the Holocene.
- The different proxies used, in particular the IRD concentration, allowed for the identification of two intervals of iceberg calving during deglaciation, at ~17.8 and ~16.9 ka cal. BP. These occurred within the period when meltwater released by the demise of the BIIS resulted in the deposition of thick plumites on the DBF. The provenance of the IRD record, based on the lithic grains petrologies, suggest European Ice Sheet calving events, including from the Hebrides and Western Scotland.
- During the Younger Dryas, an IRD-rich interval is related to a marine re-advance and calving of the Scandinavian Ice Sheet, on the basis of similar composition in the lithic grains petrologies and the recorded marine extension for SIS at that time.
- The transition into post-glacial conditions is marked by the restoration of oceanic currents and deposition of contourites. The identification of the ichnofacies *Zoophycos* in this interval marks the transition between stadial and interstadial climatic conditions, as observed elsewhere in the North Atlantic. It appears that contouritic lithofacies rich in *Zoophycos* represent a useful climatic tool in the study of the sediment record on continental margins around the North Atlantic.
- The British-Irish Ice Sheet's meltwater pulses and calving events recorded in the DBF sediments appear to be largely synchronous with those of the European Ice Sheet during the Late Quaternary and in particular at the transition between Marine Isotopic Stages 2 and 1.

This strongly suggests that such a synchronous behavior with the release of large amounts of freshwater could have had an active role on the reduction of the Atlantic Meridional Oceanic Current at this time and its effect on the North Atlantic climate.

Acknowledgments

ST acknowledges Ulster University's Vice-Chancellor Research Scholarship for support to her PhD 2014-2017. This research was funded by the UK Natural Environment Research Council grant NE/J007196/1 'BRITICE-CHRONO'. We thank the officers and crew of the *RRS James Cook* for their help with data acquisition. We also thank Stephen Livingstone, Kasper Weilbach, Riccardo Arosio, Catriona Purcell, Zoe Roseby and Elke Hanenkamp for their scientific support on the JC106 Leg 2 cruise. Thanks to Ruth Plets and William Austin for the discussion during the PhD viva and all comments they provided to an earlier version of the manuscript included in ST's thesis. The work was supported by the NERC Radiocarbon Facility (Allocation No. 1722.0613 and 1878.1014).

References

Adams, J., Maslin, M., Thomas, E., 1999. Sudden climate transitions during the Quaternary. Progress in Physical Geography, 23(1), 1-36.

Aksu, A.E., Hiscott, R.N., 1989. Slides and debris flows on the high-latitude continental slope of Baffin Bay. Geology, 17(10), 885-888.

Alley, R.B., 2000. The Younger Dryas cold interval as viewed from central Greenland. Quaternary Science Reviews, 19(1–5), 213-226.

Andrews, J.T., 2000. Icebergs and iceberg rafted detritus (IRD) in the North Atlantic: facts and assumptions. Oceanography, 13,3/2000, 100-108.

Armishaw, J.E., Holmes, R.W., Stow, D.A.V., 1998. Morphology and sedimentation on the Hebrides Slope and Barra Fan, NW UK continental margin. Geological Processes on Continental Margins: Sedimentation, Mass-Wasting and Stability. Geological Society, London, Special Publications, 129, 81-104.

Austin, W. E. N., Kroon, D., 2001. Deep sea ventilation of the northeastern Atlantic during the last 15,000 years. Global and Planetary Change, 30(1-2), 13-31.

Ballantyne, C.K., O Cofaigh, C., 2017. The last Irish Ice Sheet: extent and chronology. Advances in Irish Quaternary Studies, *1*, *101*-149.

Benetti, S., 2006. Late Quaternary sedimentary processes along the western North Atlantic margin. Ph.D. thesis, Graduate School of the National Oceanography Centre, Southampton, U.K., 204 p.

Benetti, S., Dunlop, P., Ó Cofaigh, C., 2010. Glacial and glacially-related geomorphology of the north-west Irish continental margin. Journal of Maps, 30-39.

Bigg, G.R., Clark, C.D., Greenwood, S.L., Haflidason, H., Hughes, A.L.C., Levine, R.C., Nygård, A., Sejrup, H.P., 2012. Sensitivity of the North Atlantic circulation to break-up of the marine sectors of the NW European ice sheets during the last Glacial: A synthesis of modelling and palaeoceanography. Global and Planetary Change, 98–99, 153-165.

Bond, G.C., Broecker, W., Johnsen, S., McManus, J., Labeyrie, L., Jouzel, J., Bonani, G., 1993. Correlations between climate records from North Atlantic sediments and Greenland ice. Letters to Nature, 365, 143-147.

Bradwell, T., Stoker, M.S., Golledge, N.R., Wilson, C.K., Merritt, J.W., Long, D., Everest, J.D., Hestvik, O.B., Stevenson, A.G., Hubbard, A.L., Finlayson, A.G., Mathers, H.E., 2008. The northern sector of the last British Ice Sheet: Maximum extent and demise. Earth-Science Reviews, 88(3–4), 207-226.

Broecker, W.S., Denton, G.H., Edwards, R.L. and Cheng, H., Alley, R.B., Putnam, A.E., 2010. Putting the Younger Dryas cold event into context. Quaternary Science Reviews, 29(9–10), 1078-1081.

Buckley, D.E., MacKinnon, W.G., Cranston, R.E. and Christian, H.A., 1994. Problems with piston core sampling: Mechanical and geochemical diagnosis. Marine Geology, 117(1-4), 95-106.

Callard, S.L., Ó Cofaigh, C., Benetti, S., Chiverrell, R.C., Van Landeghem, K. J.J., Saher, M.H., Gales J.A., Small, D., Clark, C.D., Livingstone, S.J., Fabel, D., Moreton, S.G., 2019. Extent and retreat history of the Barra Fan Ice Stream offshore western Scotland and northern Ireland during the last glaciation. Submitted to Quaternary Science Reviews.

Chiverrell, R.C., Thomas, G.S.P., 2010. Extent and timing of the Last Glacial Maximum (LGM) in Britain and Ireland: a review. Journal of Quaternary Science, 25(4), 535-549.

Clark, C.D., Hughes, A.L.C., Greenwood, S.L., Jordan, C., Sejrup, HP., 2012. Pattern and timing of retreat of the last British-Irish Ice Sheet. Quaternary Science Reviews, 44, 112-146.

Cronin, B.T., Akhmetzhanov, A.M., Mazzini, A., Akhmanov, G., Ivanov, M., Kenyon, N.H., 2005. Morphology, evolution and fill: Implications for sand and mud distribution in filling deep-water canyons and slope channel complexes. Sedimentary Geology, 179(1), 71-97.

Dahlgren, K.T., Vorren, T.O., 2003. Sedimentary environment and glacial history during the last 40 ka of the Vøring continental margin, mid-Norway. Marine Geology, 193(1-2), 93-127.

Davidson, S., Stoker, M.S., 2002. Late Pleistocene glacially-influenced deep-marine sedimentation off NW Britain: implications for the rock record. Geological Society, London, Special Publications, 203(1), 129-147.

Dickson, R.R., Kidd, R.B., 1987. Deep circulation in the southern Rockall Trough-the oceanographic setting of site-610. Initial Reports of the Deep Sea Drilling Project, 94, 1061-1074.

Dorador, J., Wetzel, A., Rodríguez-Tovar, F.J., 2016. *Zoophycos* in deep-sea sediments indicates high and seasonal primary productivity: Ichnology as a proxy in palaeoceanography during glacial–interglacial variations. Terra Nova, 28(5), 323-328.

Dove, D., Arosio, R., Finlayson, A., Bradwell, T., Howe, J.A., 2015. Submarine glacial landforms record Late Pleistocene ice-sheet dynamics, Inner Hebrides, Scotland. Quaternary Science Reviews, 123, 76-90.

Dowdeswell, J.A., Elverhfi, A., Spielhagen, R., 1998. Glacimarine sedimentary processes and facies on the polar north Atlantic margins. Quaternary Science Reviews, 17(1), 243-272.

Dunlop, P., Shannon, R., McCabe, M., Quinn, R., Doyle, E., 2010. Marine geophysical evidence for ice sheet extension and recession on the Malin Shelf: New evidence for the western limits of the British Irish Ice Sheet. Marine Geology, 276, 86-99.

Evans, J., Dowdeswell, J.A., Grobe, H., Niessen, F., Stein, R., Hubberten, H-W., Whittington, R.J., 2002. Late Quaternary sedimentation in Kejser Franz Joseph Fjord and the continental margin of east Greenland. Geological Society, London, Special Publications, 203(1), 149-179.

Faugeres, J.C, Gonthier, E., Grousset, F., Poutiers, J., 1981. The Feni Drift: The importance and meaning of slump deposits on the eastern slope of the Rockall Bank. Marine Geology, 40(3), M49-M57.

Finlayson, A., Fabel, D., Bradwell, T. and Sugden, D., 2014. Growth and decay of a marine terminating sector of the last British–Irish Ice Sheet: a geomorphological reconstruction. Quaternary Science Reviews, 83, 28-45.

García, M., Ercilla, G., Alonso, B., Casas, D., Dowdeswell, J.A., 2011. Sediment lithofacies, processes and sedimentary models in the Central Bransfield Basin, Antarctic Peninsula, since the Last Glacial Maximum. Marine Geology, 290(1), 1-16.

Georgiopoulou, A., Benetti, S., Shannon, P., Haughton, P.D.W., McCarron, S., 2012. Gravity flow deposits in the deep Rockall Trough, northeast Atlantic. In: Yamada, Y.e.a. ed. Submarine mass movements and their consequences, Advances in natural and technological hazards research. 31st ed. Netherlands: Springer, 695-707.

Haapaniemi, A.I., Scourse, J.D., Peck, V.L., Kennedy, H., Kennedy, P., Hemming, S.R., Furze, M.F.A., Pienkowski, A.J., Austin, W.E.N., Walden, J., Wadsworth, E., Hall, I.R., 2010. Source, timing, frequency and flux of ice-rafted detritus to the Northeast Atlantic margin, 30-12 ka: testing the Heinrich precursor hypothesis. Boreas an International Journal of Quaternary Research, 39, 576-591.

Heinrich, H., 1988. Origin and consequences of cyclic ice rafting in the Northeast Atlantic Ocean during the past 130,000 years. Quaternary Research, 29(2), 142-152.

Hesse, R., Khodabakhsh, S., Klaucke, I., Ryan, W.B.F., 1997. Asymmetrical turbid surface-plume deposit near ice-outlets of the Pleistocene Laurentide ice sheet in the Labrador Sea. Geo-Marine Letters, 17(3), 179-187.

Hesse, R., Klauck, I., Khodabakhsh, S., Piper, D., 1999. Continental slope sedimentation adjacent to an ice margin. III. The upper Labrador Slope. Marine Geology, 155(3–4), 249-276.

Hjelstuen, B.O., Haflidason, H., Sejrup, H.P., Lyså, A., 2009. Sedimentary processes and depositional environments in glaciated fjord systems - Evidence from Nordfjord, Norway. Marine Geology, 258(1-4), 88-99.

Holliday, P.N., Pollard, R.T., Read, J.F., Leach, H., 2000. Water mass properties and fluxes in the Rockall Trough, 1975–1998. Deep Sea Research Part I: Oceanographic Research Papers, 47(7), 1303-1332.

Holmes, R., Long, D., Dodd, L.R., 1998. Large-scale debrites and submarine landslide on the Barra Fan, west of Britain. Geological Processes on Continental Margins: Sedimentation, Mass-Wasting and Stability. Geological Society, London, Special Publications, 129, 67-79.

Howe, J.A., 1995. Sedimentary processes and variations in slope-current activity during the last Glacial-Interglacial episode on the Hebrides Slope, northern Rockall Trough, North Atlantic Ocean. Sedimentary Geology, 96(3), 201-230.

Howe, J.A., 1996. Turbidite and contourite sediment waves in the northern Rockall Trough, North Atlantic Ocean. Sedimentology, 43, 219-234.

Howe, J.A., Harland, R., Hine, N.M., Austin, W.E.N., 1998. Late Quaternary stratigraphy and palaeoceanographic change in the northern Rockall Trough, North Atlantic Ocean. Geological Processes on Continental Margins: Sedimentation, Mass-Wasting and Stability. Geological Society, London, Special Publications, 129, 269-286.

Howe, J.A., Dove, D., Bradwell, T., Gafeira, J., 2012. Submarine geomorphology and glacial history of the Sea of the Hebrides, UK. Marine Geology, 315-318(Supplement C), 64-76.

Hughes, A.L.C., Gyllencreutz, R., Lohne O.S., Mangerud, J., Svendesen J.I., 2015. The last Eurasian Ice Sheet - a chronological database and time-slice reconstruction, DATED-1. Boreas an International Journal of Quaternary Research, 45, 1-45.

Jessen, S.P., Rasmussen, T.L., Nielsen, T., Solheim, A., 2010. A new Late Weichselian and Holocene marine chronology for the western Svalbard slope 30,000–0 cal years BP. Quaternary Science Reviews, 29(9-10), 1301-1312.

Knutz, P.C., Austin, W.E.N., Jones, E.J.W., 2001. Millennial-scale depositional cycles related to British Ice Sheet variability and North Atlantic palaeocirculation since 45 kyrs B.P., Barra fan, U.K. margin. Paleoceanography, 16, 53-64.

Knutz, P.C., Jones, E.J.W., Austin, W.E.N., van Weering, T.C.E., 2002. Glacimarine slope sedimentation, contourite drifts and bottom current pathways on the Barra Fan, UK North Atlantic margin. Marine Geology, 188(1–2), 129-146.

Lekens, W.A.H., Sejrup, H.P., Haflidason, H., Petersen, G.Ø., Hjelstuen, B., Knorr, G., 2005. Laminated sediments preceding Heinrich event 1 in the Northern North Sea and Southern Norwegian Sea: origin, processes and regional linkage. Marine Geology, 216(1-2), 27-50.

Lisiecki, L. E., Raymo, M.E., 2005. A Pliocene-Pleistocene stack of 57 globally distributed benthic δ18O records. Paleoceanography, 20(1), PA1003.

Lowe, D.R., 1979. Sediment gravity flows: their classification and some problems of application to natural flows and deposits. In: Doyle, L.J., Pilkey, O.H. ed. Geology of continental slopes. Special Publication, 27 ed. Tulsa, Oklahoma: Society of economic paleontologists and mineralogists, 75-84.

Lowe, D.R., 1982. Sediment gravity flows: II. Depositional models with special reference to the deposits of high density turbidity currents. Journal of Sedimentary Petrology, 52, 279-297.

Löwemark, L., Lin, H.L., Sarnthein, M., 2006. Temporal variations of the trace fossil *Zoophycos* in a 425 ka long sediment record from the South China Sea: implications for the ethology of the *Zoophycos* producer. Geological Magazine, 143(1), 105-114.

Lucchi, R.G., Rebesco, M., Camerlenghi, A., Busetti, M., Tomadin, L., Villa, G., Persico, D., Morigi, C., Bonci, M.C., Giorgetti, G., 2002. Mid-late Pleistocene glacimarine sedimentary processes of a high-latitude, deep-sea sediment drift (Antarctic Peninsula Pacific margin). Marine Geology, 189(3–4), 343-370.

Lucchi, R.G., Sagnotti, L., Camerlenghi, A., Macrì, P., Rebesco, M., Pedrosa, M.T., Giorgetti, G., 2015. Marine sedimentary record of Meltwater Pulse 1a along the NW Barents Sea continental margin. arktos, 1(1), 7.

Lynch-Stieglitz, J., Schmidt, M.W., Curry, W.B., 2011. Evidence from the Florida Straits for Younger Dryas ocean circulation changes. Paleoceanography, 26(1), PA1205.

Mangerud, J., Aarseth, I., Hughes, A.L.C., Lohne, Ø.S., Skår, K., Sønstegaard, E., Svendsen, J.I., 2016. A major re-growth of the Scandinavian Ice Sheet in western Norway during Allerød-Younger Dryas. Quaternary Science Reviews, 132, 175-205.

Masson, D.G., Plets, R.M.K., Huvenne, V.A.I., Wynn, R.B., Bett, B.J., 2010. Sedimentology and depositional history of Holocene sandy contourites on the lower slope of the Faroe–Shetland Channel, northwest of the UK. Marine Geology, 268(1), 85-96.

McCartney, M.S., 1992. Recirculating components to the deep boundary current of the northern North Atlantic. Progress in Oceanography, 29(4), 283-383.

McManus, J.F., Francois, R., Gherardi, J.M., Keigwin, L.D., Brown-Leger, S., 2004. Collapse and rapid resumption of Atlantic meridional circulation linked to deglacial climate change. Letter to Nature, 428, 834-837.

Middleton, G.V., Hampton, M.A., 1976. Subaqueous sediment transport and deposition by sediment gravity flows. Marine Sediment Transport (Eds.D.J.Stanley and D.J.P.Swift), 197-218. Wiley, New York.

Mingard, K., Morrell, R., Jackson, P., Lawson, S., Patel, S., Buxton, R., 2009. Good practice guide for improving the consistency of particle size measurements.

Mitchum, R.M., Vail, P.R., Sangree, J.B., 1977. Seismic stratigraphy and global changes of sea level: Part 6. Stratigraphic interpretation of seismic reflection patterns in depositional sequences: Section 2. Application of seismic reflection configuration to stratigraphic interpretation. In: Anon. Seismic stratigraphy- applications to hydrocarbon exploration. AAPG Special Volumes, 117-133.

New, A.L., Smythe-Wright, D., 2001. Aspects of the circulation in the Rockall Trough. Continental Shelf Research, 21(8–10), 777-810.

Ó Cofaigh, C., Dowdeswell, J.A., 2001. Laminated sediments in glacimarine environments: diagnostic criteria for their interpretation. Quaternary Science Reviews, 20(13), 1411-1436.

Ó Cofaigh, C., Dunlop, P., Benetti, S., 2012. Marine geophysical evidence for Late Pleistocene ice sheet extent and recession off northwest Ireland. Quaternary Science Reviews, 44, 147-159.

O'Reilly, B.M., Shannon, P.M., Readman, P.W., 2007. Shelf to slope sedimentation processes and the impact of Plio–Pleistocene glaciations in the northeast Atlantic, west of Ireland. Marine Geology, 238(1), 21-44.

Owen, M.J., Maslin, M.A., Day, S.J. and Long, D., 2018. Sediment failures within the Peach Slide (Barra Fan, NE Atlantic Ocean) and relation to the history of the British-Irish Ice Sheet. Quaternary Science Reviews, 187, 1-30.

Peck, V.L., Hall, I.R., Zahn, R., Elderfield, H., Grousset, F., Hemming, S.R., Scourse, J.D., 2006. High resolution evidence for linkages between NW European ice sheet instability and Atlantic Meridional Overturning Circulation. Earth and Planetary Science Letters, 243(3–4), 476-488.

Peck, V.L., Hall, I.R., Zahn, R., Grousset, F., Hemming, S.R., Scourse, J.D., 2007. The relationship of Heinrich events and their European precursors over the past 60 ka BP: a multi-proxy ice-rafted debris provenance study in the North East Atlantic. Quaternary Science Reviews, 26(7–8), 862-875.

Peters, J.L, Benetti, S., Dunlop, P., Ó Cofaigh, C., 2015. Maximum extent and dynamic behaviour of the last British–Irish Ice Sheet west of Ireland. Quaternary Science Reviews, 128, 48-68.

Piper, D.J. (1988) DNAG# 3. Glaciomarine sedimentation on the continental slope off eastern Canada. Geoscience Canada, 15(1).

Piper, D.J.W., 2005. Late Cenozoic evolution of the continental margin of eastern Canada. Norwegian Journal of Geology, 85, 305-318.

Piper, D.J. and Normark, W.R., 2009. Processes that initiate turbidity currents and their influence on turbidites: a marine geology perspective. Journal of Sedimentary Research, 79(6), 347-362.

Prothro, L.O., Simkins, L.M., Majewski, W., Anderson, J.B., 2018. Glacial retreat patterns and processes determined from integrated sedimentology and geomorphology records. Marine Geology, 395, 104-119.

Rahmstorf, S., 2002. Ocean circulation and climate during the past 120,000 years. Nature, 419(6903), 207-214.

Ramsey, C.B., 2009. Bayesian analysis of radiocarbon dates. Radiocarbon, 51(1), 337-360.

Rasmussen, S.O., Bigler, M., Blockley, S.P., Blunier, T., Buchardt, S.L., Clausen, H.B., Cvijanovic, I., Dahl-Jensen, D., Johnsen, S.J., Fischer, H., Gkinis, V., Guillevic, M., Hoek, W.Z., Lowe, J.J., Pedro, J.B., Popp, T., Seierstad, I.K., Steffensen, J.P., Svensson, A.M., Vallelonga, P., Vinther, B.M., Walker, M.J.C., Wheatley, J.J., Winstrup, M., 2014. A stratigraphic framework for abrupt climatic changes during the Last Glacial period based on three synchronized Greenland ice-core records: refining and extending the INTIMATE event stratigraphy. Quaternary Science Reviews, 106(Supplement C), 14-28.

Read, J.F., 2000. CONVEX-91: water masses and circulation of the Northeast Atlantic subpolar gyre. Progress in Oceanography, 48(4), 461-510.

Rebesco, M., Hernández-Molina, F.J., Van Rooij, D., Wåhlin, A., 2014. Contourites and associated sediments controlled by deep-water circulation processes: State-of-the-art and future considerations. Marine Geology, 352, 111-154.

Reimer, P.J., Bard, E., Bayliss, A., Beck, J.W., Blackwell, P.G., Ramsey, C.B.,Buck, C.E., Cheng, H., Edwards, R.L., Friedrich, M., Grootes, P.M., Guilderson, T.P., Haflidason, H., Hajdas, I., Hatté, C., Heaton, T.J., Hoffmann, D.L., Hogg, A.G., Hughen, K.A., Kaiser, K.F., Kromer, B., Manning, S.W., Niu, M., Reimer, R.W., Richards, D.A., Scott, E.M., Southon, J.R., Staff, R.A., Turney, C.S.M., van der Plicht, J., 2013. IntCal13 and Marine13 Radiocarbon Age Calibration Curves 0–50,000 Years cal BP. Radiocarbon, 55(4), 1869-1887.

Roger, J., Saint-Ange, F., Lajeunesse, P., Duchesne, M.J., St-Onge, G., 2013. Late Quaternary glacial history and meltwater discharge along the northestern Newfoundland shelf. Canadian Journal of Earth Sciences, 50, 1178-1194.

Rørvik, K.L., Laberg, J.S., Hald, M., Ravna, E.K., Vorren, T.O., 2010. Behavior of the northwestern part of the Fennoscandian Ice Sheet during the Last Glacial Maximum–a response to external forcing. Quaternary Science Reviews, 29(17-18), 2224-2237.

Sacchetti, F., Benetti, S., Georgiopoulou, A., Shannon, P.M., O'Reilly, B.M., Dunlop, P., Quinn, R., Ó Cofaigh, C., 2012a. Deep-water geomorphology of the glaciated Irish margin from high-resolution marine geophysical data. Marine Geology, 291–294, 113-131.

Sacchetti, F., Benetti, S., Ó Cofaigh, C., Georgiopoulou, A., 2012b. Geophysical evidence of deep-keeled icebergs on the Rockall Bank, Northeast Atlantic Ocean. Geomorphology, 159–160, 63-72.

Scourse, J.D., Haapaniemi, A.I., Colmenero-Hidalgo, E., Peck, V.L., Hall, I.R., Austin, W.E.N., Knutz, P.C., Zahn, R., 2009. Growth, dynamics and deglaciation of the last British–Irish ice sheet: the deep-sea ice-rafted detritus record. Quaternary Science Reviews, 28(27–28), 3066-3084.

Sejrup, H-P., Hjelstuen, B.O., Torbjørn, D.K.I., Haflidason, H., Kuijpers, A., Nygård, A., Praeg, S., Stoker, M.S., Vorren, T.O., 2005. Pleistocene glacial history of the NW European continental margin. Marine and Petroleum Geology, 22(9–10), 1111-1129.

Small, D., Rinterknecht, V., Austin, W.E., Bates, R., Benn, D.I., Scourse, J.D., Bourlès, D.L., Hibbert, F.D. and ASTER Team, 2016. Implications of 36Cl exposure ages from Skye, northwest Scotland for the timing of ice stream deglaciation and deglacial ice dynamics. Quaternary Science Reviews, 150,130-145.

Small, D., Benetti, S., Dove, D., Ballantyne, C.K., Fabel, D., Clark, C.D., Gheorghiu, D.M., Newall, J., Xu, S., 2017. Cosmogenic exposure age constraints on deglaciation and flow behaviour of a marine-based ice stream in western Scotland, 21–16 ka. Quaternary Science Reviews, 167, 30-46.

Stanford, J.D., Rohling, E.J., Bacon, S., Roberts, A.P., Grousset, F.E., Bolshaw, M., 2011. A new concept for the paleoceanographic evolution of Heinrich event 1 in the North Atlantic. Quaternary Science Reviews, 30(9–10), 1047-1066.

Stoker, M.S., 1995. The influence of glacigenic sedimentation on slope-apron development on the continental margin off Northwest Britain. The Tectonics, Sedimentation and Palaeoceanography of the North Atlantic Region, Geological Society Special Publication, 90, 159-177.

Stoker, M.S., 1997. Mid- to la Cenozoic sedimentation on the continental margin off NW Britain. Journal of the Geological Society, London, 154, 509-515.

Stoker, M.S., Leslie, A.B., Scott, W.D., Briden, J.C., Hine, N.M., Harland, R., Wilkinson, I.P., Evans, D., Ardus, D.A., 1994. A record of late Cenozoic stratigraphy, sedimentation and climate change from the Hebrides Slope, NE Atlantic Ocean. Journal of the Geological Society, 151(2), 235-249.

Stoker, M.S., Praeg, D., Hjelstuen, B.O., Laberg, J.S., Nielsen, T., Shannon, P.M., 2005. Neogene stratigraphy and the sedimentary and oceanographic development of the NW European Atlantic margin. Marine and Petroleum Geology, 22(9–10), 977-1005.

Stow, D.A.V., 1979. Distinguishing between fine-grained turbidites and contourites on the Nova Scotia deep water margin. Sedimentology, 26, 371-387.

Stow, D.A.V., Lovell, J.P.B., 1979. Contourites: Their recognition in modern and ancient sediments. Earth-Science Reviews, 14(3), 251-291.

Stow, D.A.V., Piper, D.J.W., 1984. Deep-water fine-grained sediments: facies models. Fine-Grained Sediments: Deep Water Processes and Facies. Blackwell Scientific Publication for the Geological Society, 661-644.

Stow, D.A.V., Reading, H.G., Collinson, J.D., 1996. Deep seas. Sedimentary Environments: Processes, Facies and Stratigraphy, 3, 395-453.

Stow, D.A.V., Mayall, M., 2000. Deep-water sedimentary systems: New models for the 21st century. Marine and Petroleum Geology, 17(2), 125-135.

Stow, D.A.V., Faugeres, J-C., Howe, J.A., Pudsey, C.J., Viana, A.R., 2002. Bottom currents, contourites and deep-sea sediment drift: current state-of-the-art. Deep-Water Contourite Systems: Modern Drifts and Ancient Series, Seismic and Sedimentary Characteristics. Geological Society, London, Memoirs, 22, 7-20.

Toucanne, S., Soulet, G., Freslon, N., Silva Jacinto, R., Dennielou, B., Zaragosi, S., Eynaud, F., Bourillet, J.F., Bayon, G., 2015. Millennial-scale fluctuations of the European Ice Sheet at the end of the last glacial, and their potential impact on global climate. Quaternary Science Reviews, 123, 113-133.

Tripsanas, E.K., Piper, D.J.W., 2008. Glaciogenic debris-flow deposits of Orphan Basin, offshore eastern Canada: sedimentological and rheological properties, origin, and relationship to meltwater discharge. Journal of Sedimentary Research, 78(11), 724-744.

Van Landeghem, K.J., Wheeler, A.J., Mitchell, N.C., 2009. Seafloor evidence for palaeo-ice streaming and calving of the grounded Irish Sea Ice Stream: Implications for the interpretation of its final deglaciation phase. Boreas, 38, 119-131.

Wanamaker Jr, A.D., Butler, P.G., Scourse, J.D., Heinemeier, J., Eiríksson, J., Knudsen, K.L., Richardson, C.A., 2012. Surface changes in the North Atlantic meridional overturning circulation during the last millennium. Nature Communications, 3, 899.

Wang, D., Hesse, R., 1996. Continental slope sedimentation adjacent to an ice-margin. II. Glaciomarine depositional facies on labrador slope and glacial cycles. Marine Geology, 135(1), 65-96.

Weaver, P.P.E., Wynn, R.B., Kenyon, N.H., Evans, J., 2000. Continental margin sedimentation, with special reference to the north-east Atlantic margin. Sedimentology, 47(s1), 239-256.

Wilson, L.J., Austin, W.E.N., Jansen, E., 2002. The last British Ice Sheet: growth, maximum extent and deglaciation. Polar Research, 21(2), 243-250.

Wynn, R.B., Stow, D.A.V., 2002. Classification and characterisation of deep-water sediment waves. Marine Geology, 192(1), 7-22.

Figure 1: North Atlantic glaciated margin with the highlighted approximate extent of the Donegal Barra fan and JC106 core locations. The main direction of ice-streaming during the last glacial period is indicated by the black arrows (Hebrides Ice Stream-HIS; North Channel Ice Stream-NCIS). Inset shows the position of the main map along the Atlantic margin with the main water masses. The bathymetry data is supplied by the GEBCO, General Bathymetric Chart of the Ocean and the colour scale was selected for better visibility of the glacial features on the shelf. A-A': Location of seismic line presented in this paper. DBF=Donegal-Barra Fan (outline from Sacchetti et al., 2012), MSs= Malin Sea shelf, OH= Outer Hebrides, RT=Rockall Trough, HS=Hebrides Terrace Seamount, ADS=Anton Dohrn Seamount, NADW=North Atlantic Deep Water, ENAW=Eastern North Atlantic Water.

Figure 2: Seismic profile along the slope with core location for 134PC and 133PC. Insets are indicated for the a) lower slope, b) middle slope, c) upper slope. The acoustic facies identified are indicated by coloured lines.

Figure 3: Five lithofacies illustrated with x-radiographs. Foraminiferal-bearing mud: FM (identified by the yellow lateral bar); Extensively bioturbated mud: BM (Zoophycos burrows shown by orange arrows; this image is presented with inverted grey-colour scale to better display the ichnofacies); Chaotic mud: CM (purple arrow indicates an inclined shear surface); Laminated sand to mud couplet: LSM (fining upward of the sediment visible in the x-rays); Laminated mud rich in IRD: ILM (larger lithic grains indicated by blue arrows and laminations are visible in the x-rays).

Figure 4: X-radiographs, lithofacies identification, log, magnetic susceptibility (MS), mean volume grain size (μm) (D), IRD concentration [IRD], abundance of Neogloboquadrina pachyderma sinistral (%NPS calculated as percentage of the total planktonic foraminiferal assemblage) and conventional radiocarbon ages for core JC106-133PC. MS data from Figs. 4 to 6, present a wider spacing, approximately every meter, in correspondence of the end of the core sections. Lithofacies:

FM=Foraminiferal-bearing mud, BM=Extensively bioturbated mud, CM=Chaotic mud, LSM=Laminated sand to mud couplet, ILM=Laminated mud rich in IRD.

Figure 5: X-radiographs, lithofacies identification, log, magnetic susceptibility (MS), mean volume grain size (D), IRD concentration [IRD] and conventional radiocarbon age for core JC106-128PC.

Figure 6: X-radiographs, lithofacies identification, log, magnetic susceptibility (MS), mean volume grain size (D), IRD concentration [IRD] and conventional radiocarbon ages for core JC106-134PC.

Figure 7: From left to right – δ18O record from the GISP2 ice core record from Greenland (Rasmussen et al., 2014) for the last 20ka and stadials (cold/light blue) and interstadials (warm/light pink). GS: Greenland stadial; GI: Greenland interstadial; BL: Bølling-Allerød, YD: Younger Dryas. Marine Isotopic Stages (MIS) boundaries after Lisiecki & Raymo (2005). The time interval covered by the DBF sediment record is indicated and the GISP2 record for this specific interval is zoomed in. The dark blue arrow indicated the high peak in IRD concentration dated ~16.9 ka cal. BP, the light blue arrow the older rich in IRD event dated ~17.8 ka cal. BP.

Figure 8: Correlation between the three DBF sediment cores based on lithofacies, [IRD] concentration and calibrated radiocarbon dates. The yellow arrow at the 128PC core top highlights the thin FM facies.

Figure 9: Schematic depositional model for the DBF. The sedimentation is represented by meltwater pulses, iceberg discharges and downslope mass transport. Meltwater and iceberg presence are recorded in sediments older than 15.9 ka cal. BP and of Younger Dryas age. Contouritic deposition is recognised for sediment dated after 15.2 ka cal. BP. Currents abbreviations: ENAW= Eastern North Atlantic Water; DNBC= Deep Northern Boundary Current.

Table 1: Sediment core information.

Core	Latitude (°N)	Longitude (°W)	Water depth (m)	Core Length (cm)
JC106-128PC	56.17147	-9.616743	1475	668
JC106-133PC	56.44449	-9.672212	1537	661
JC106-134PC	56.44471	-9.321229	1036	672

*Table 2: Radiocarbon results. Sample indicated by * was not taken into account for age reconstruction as it was at a later stage recognized to be in a re-deposited/disturbed interval. All the values are rounded to the nearest decade or multiple of 5. NPS=Neogloboquadrina pachyderma sinistral, G.B.= Globigerina bulloides.*

Core	Depth (cm)	Sample material	^{14}C Age (yrs. BP)	Calibrated age (yrs. BP) ΔR=0	Calibrated age (yrs. BP) ΔR=300	Calibrated age (yrs. BP) ΔR=700	Surrounding lithofacies	Laboratory code
128PC	125-128	Mono. NPS	13710 ± 40	15995 ± 180	15550 ± 220	14960 ± 230	LM	SUERC-67943
134PC	60-61	Mono. G.B.	13175 ± 40	15240 ± 140	14635 ± 360	13955 ± 135	EXFM	SUERC-63572
134PC	588-593	Mixed benthic forams	15020 ± 45	17800 ± 170	17445 ± 180	16865 ± 225	LM	SUERC-63573
133PC	175-176	Mono. NPS	11200 ± 30	12690 ± 90	12440 ± 150	11655 ± 250	LM	441865
133PC	375-376*	Mixed benthic forams	15270 ± 45	18070 ± 170	17750 ± 175	17250 ± 195	SMC	SUERC-67947
133PC	433-438	Mono. NPS	14355 ± 40	16915 ± 220	16455 ± 210	15930 ± 175	LM	SUERC-67948
133PC	583-588	Mono. NPS	15050 ± 50	17825 ± 175	17465 ± 195	16885 ± 240	LM	450231

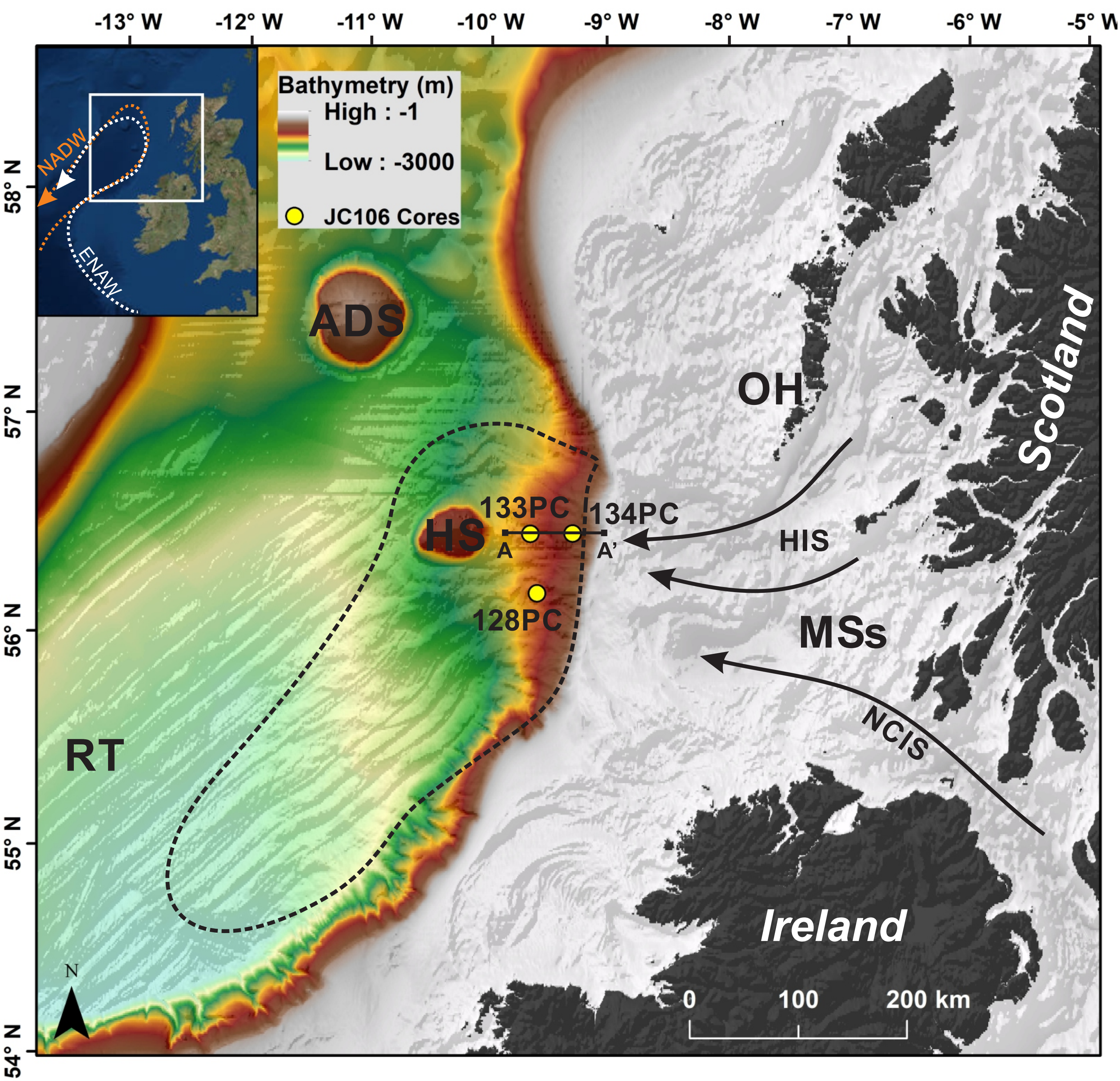
-13° W
-12° W
-11° W
-10° W
-9° W
-8° W
-7° W
-6° W
-5° W
58° N
57° N
56° N
55° N
54° N
Bathymetry (m)
High : -1
Low : -3000
JC106 Cores
NADW
ENAW
ADS
OH
Scotland
133PC
134PC
HS
A
A'
HIS
128PC
MSs
NCIS
RT
Ireland
N
0
100
200 km

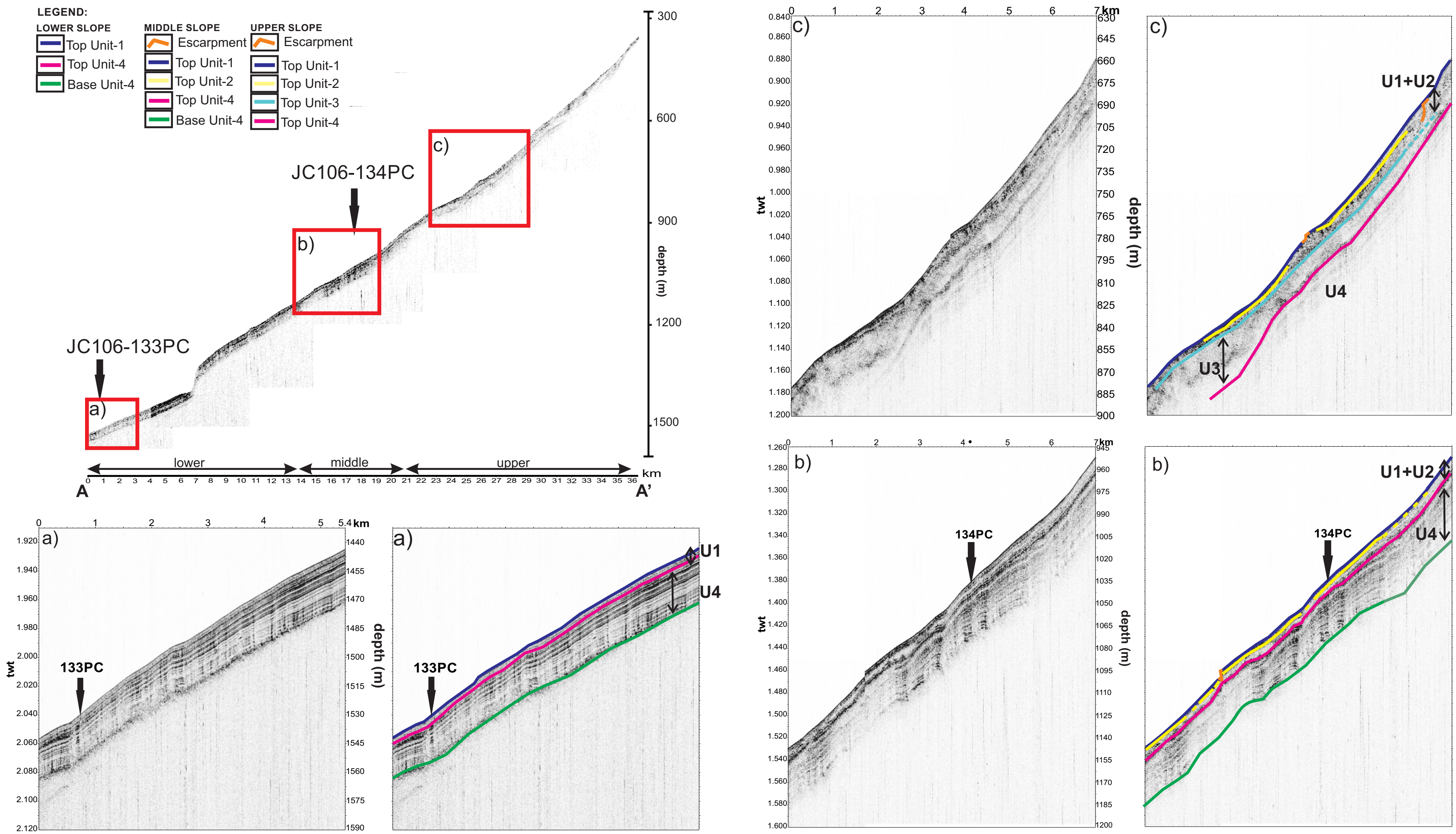
LEGEND:
LOWER SLOPE
Top Unit-1
Top Unit-4
Base Unit-4
MIDDLE SLOPE
Escarpment
Top Unit-1
Top Unit-2
Top Unit-4
Base Unit-4
UPPER SLOPE
Escarpment
Top Unit-1
Top Unit-2
Top Unit-3
Top Unit-4
JC106-134PC
JC106-133PC
a)
b)
c)
depth (m)
lower
middle
upper
km
A
A'
twt
133PC
134PC
U1
U4
U1+U2
U3

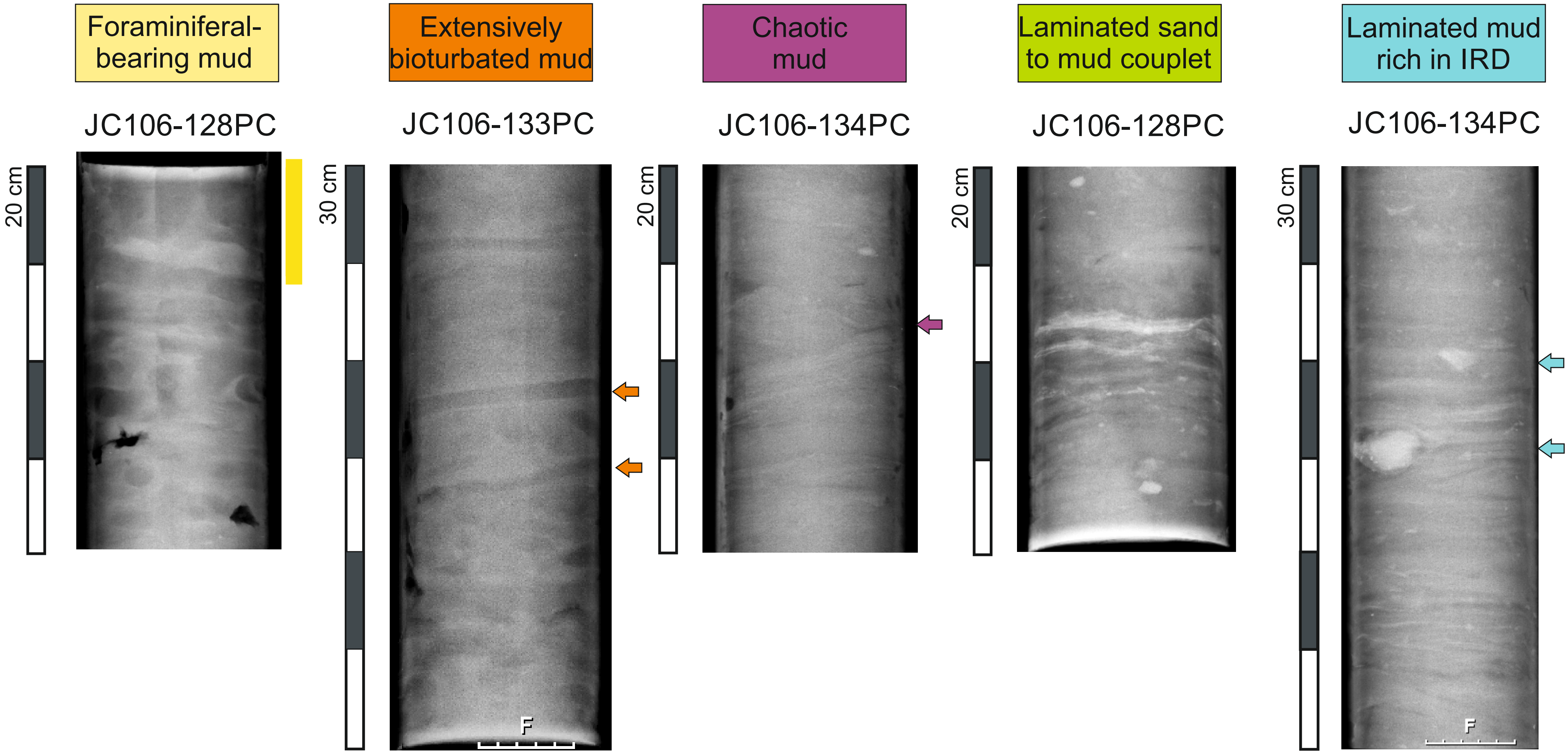
Foraminiferal-bearing mud
Extensively bioturbated mud
Chaotic mud
Laminated sand to mud couplet
Laminated mud rich in IRD
JC106-128PC
JC106-133PC
JC106-134PC
JC106-128PC
JC106-134PC
20 cm
30 cm
20 cm
20 cm
30 cm
F
F

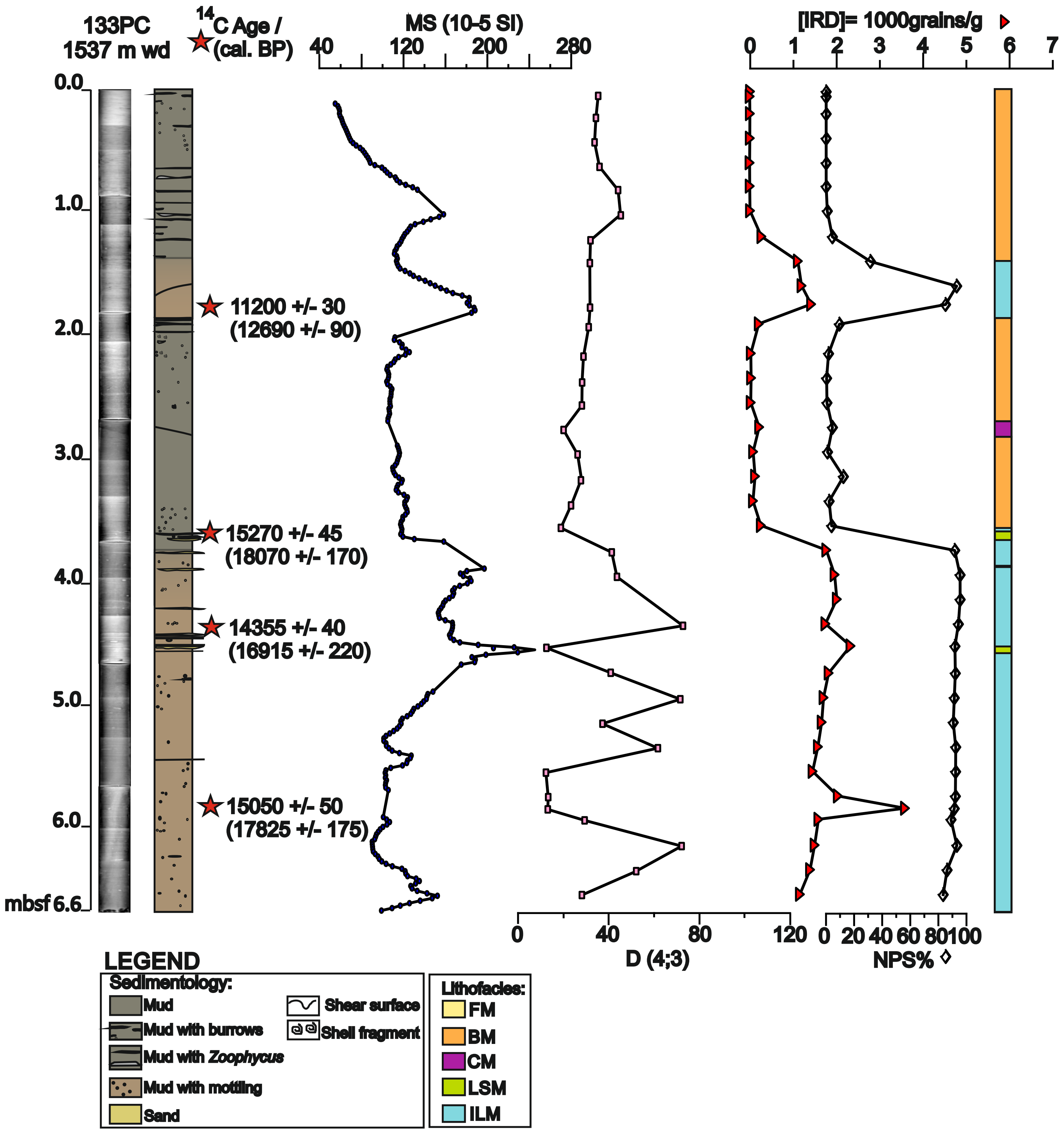
133PC
1537 m wd
14C Age / (cal. BP)
MS (10-5 SI)
40
120
200
280
[IRD]= 1000grains/g
0
1
2
3
4
5
6
7
0.0
1.0
2.0
3.0
4.0
5.0
6.0
mbsf 6.6
11200 +/- 30
(12690 +/- 90)
15270 +/- 45
(18070 +/- 170)
14355 +/- 40
(16915 +/- 220)
15050 +/- 50
(17825 +/- 175)
0
40
80
120
D (4;3)
0
20
40
60
80
100
NPS%
LEGEND
Sedimentology:
Mud
Mud with burrows
Mud with Zoophycus
Mud with mottling
Sand
Shear surface
Shell fragment
Lithofacies:
FM
BM
CM
LSM
ILM

PDF Click here to access/download;figure;Fig.5.pdf

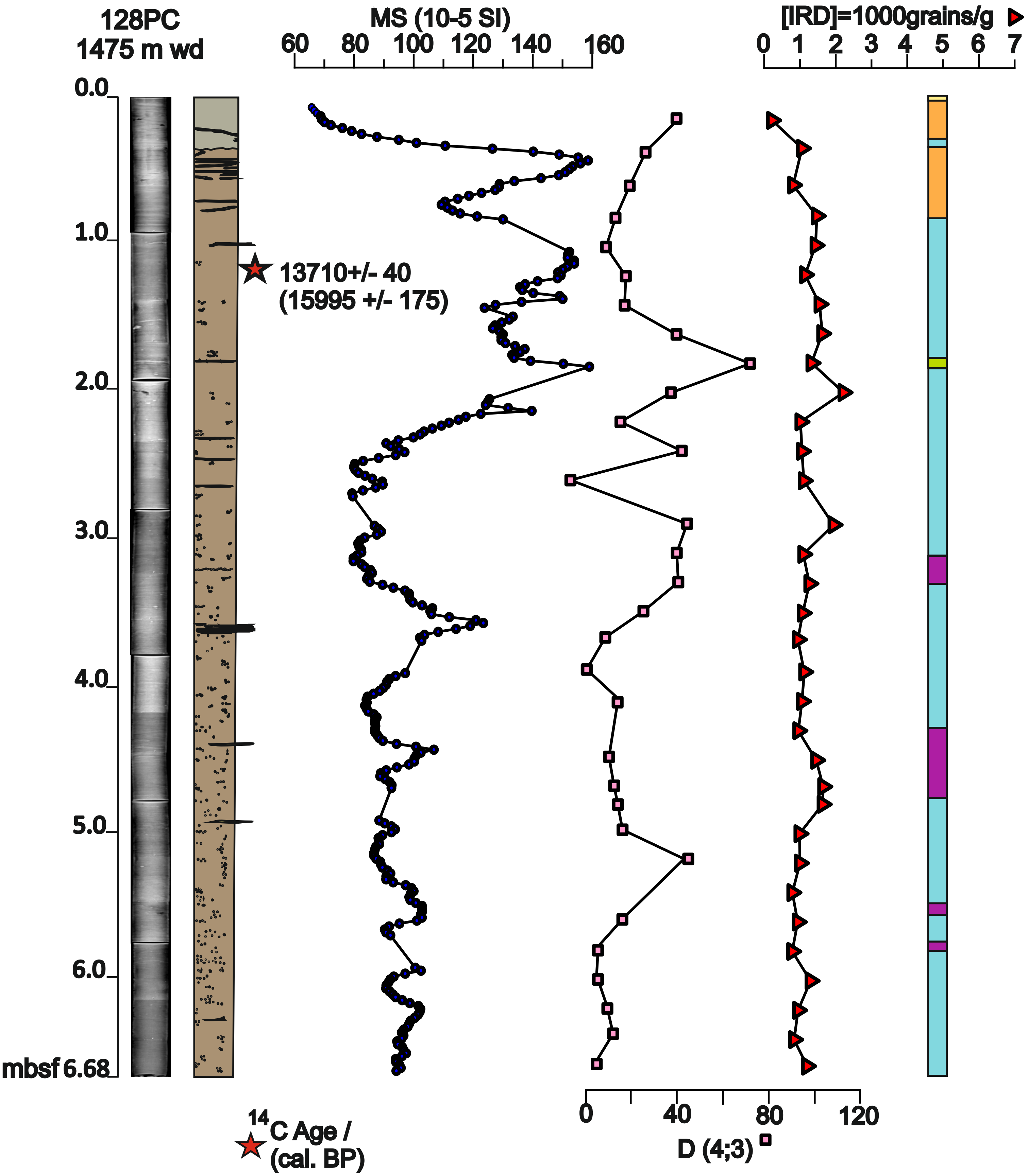

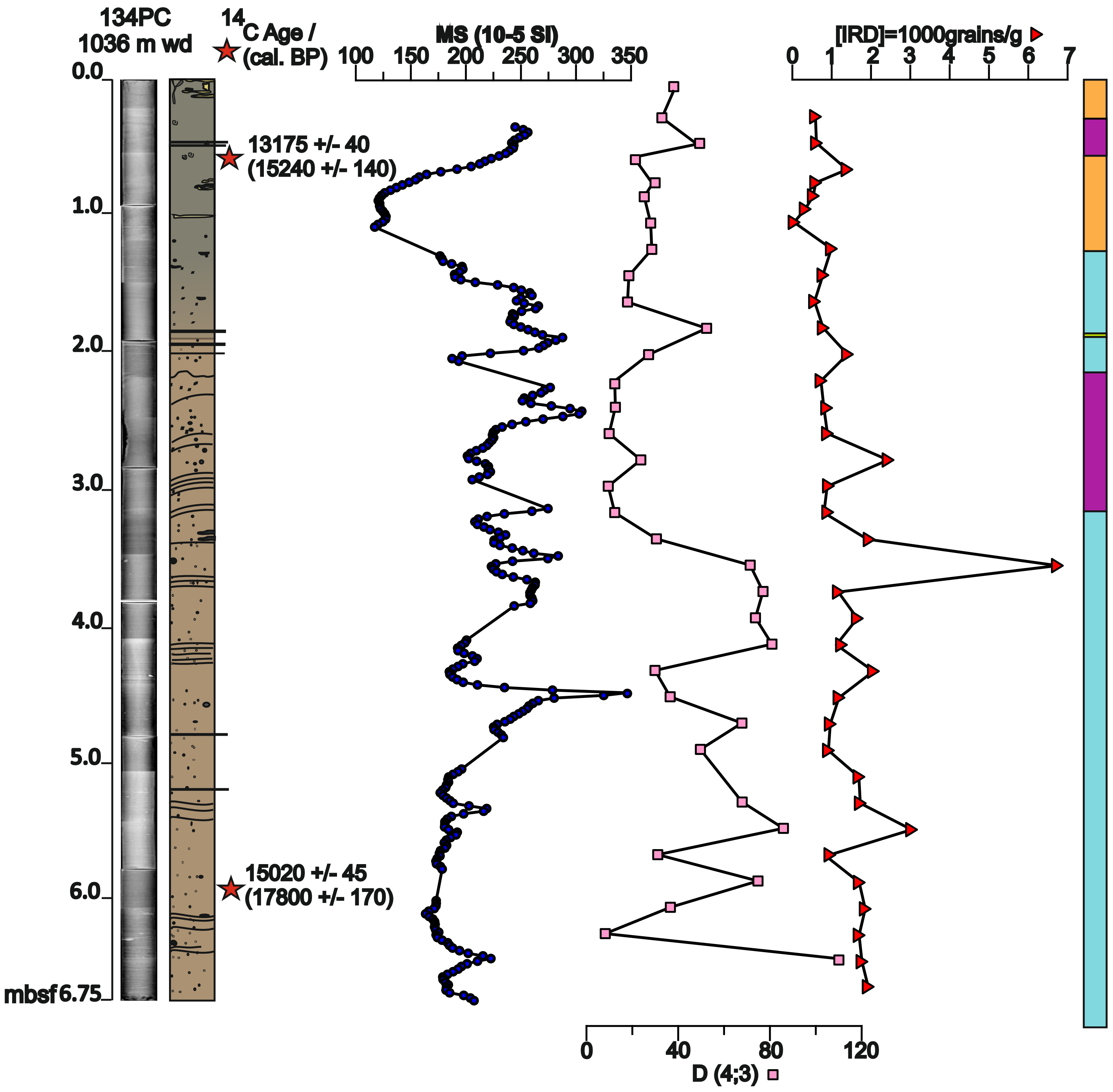
134PC
1036 m wd
14C Age /
(cal. BP)
MS (10-5 SI)
100 150 200 250 300 350
[IRD]=1000grains/g
0 1 2 3 4 5 6 7
0.0
1.0
2.0
3.0
4.0
5.0
6.0
mbsf 6.75
13175 +/- 40
(15240 +/- 140)
15020 +/- 45
(17800 +/- 170)
0 40 80 120
D (4;3)

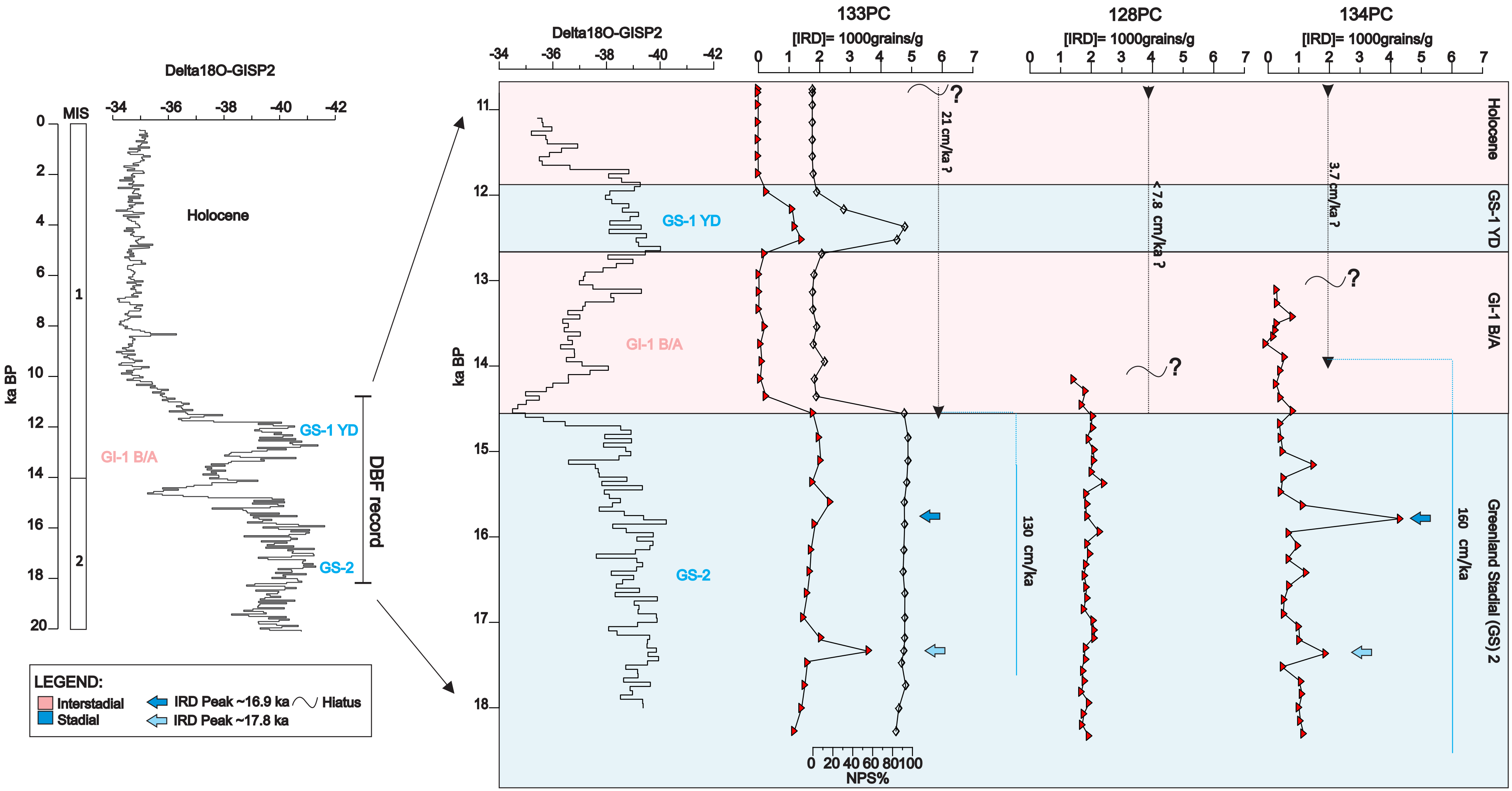
Delta18O-GISP2
MIS
ka BP
Holocene
GI-1 B/A
GS-1 YD
GS-2
DBF record
1
2
LEGEND:
Interstadial
Stadial
IRD Peak ~16.9 ka
IRD Peak ~17.8 ka
Hiatus
133PC
128PC
134PC
[IRD]= 1000grains/g
21 cm/ka ?
<7.8 cm/ka ?
3.7 cm/ka ?
130 cm/ka
160 cm/ka
NPS%
Greenland Stadial (GS) 2

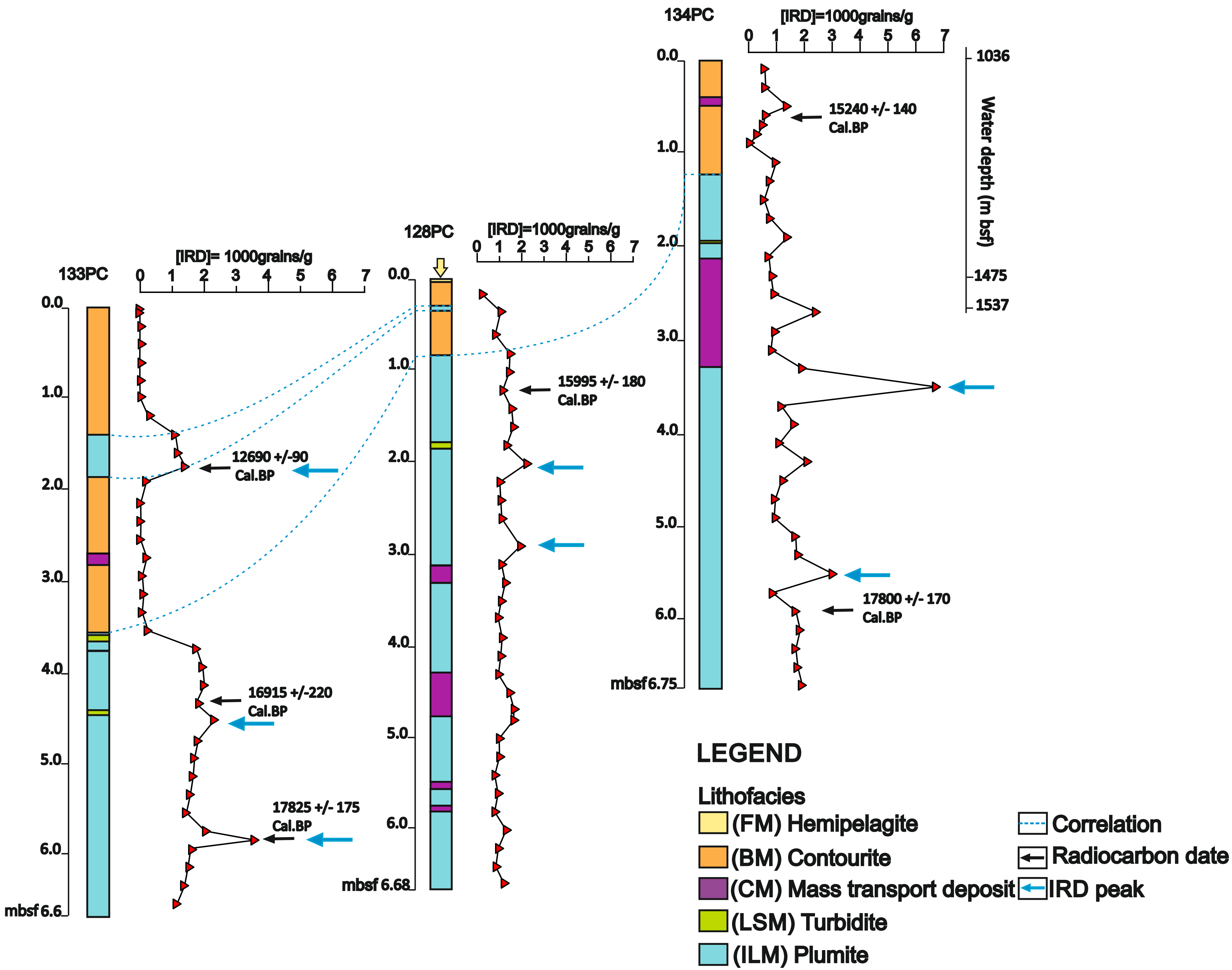
133PC
[IRD]= 1000grains/g
0 1 2 3 4 5 6 7
0.0
1.0
2.0
3.0
4.0
5.0
6.0
mbsf 6.6
12690 +/-90
Cal.BP
16915 +/-220
Cal.BP
17825 +/- 175
Cal.BP
128PC
[IRD]=1000grains/g
0 1 2 3 4 5 6 7
0.0
1.0
2.0
3.0
4.0
5.0
6.0
mbsf 6.68
15995 +/- 180
Cal.BP
134PC
[IRD]=1000grains/g
0 1 2 3 4 5 6 7
0.0
1.0
2.0
3.0
4.0
5.0
6.0
mbsf 6.75
15240 +/- 140
Cal.BP
17800 +/- 170
Cal.BP
1036
1475
1537
Water depth (m bsf)
LEGEND
Lithofacies
(FM) Hemipelagite
(BM) Contourite
(CM) Mass transport deposit
(LSM) Turbidite
(ILM) Plumite
Correlation
Radiocarbon date
IRD peak

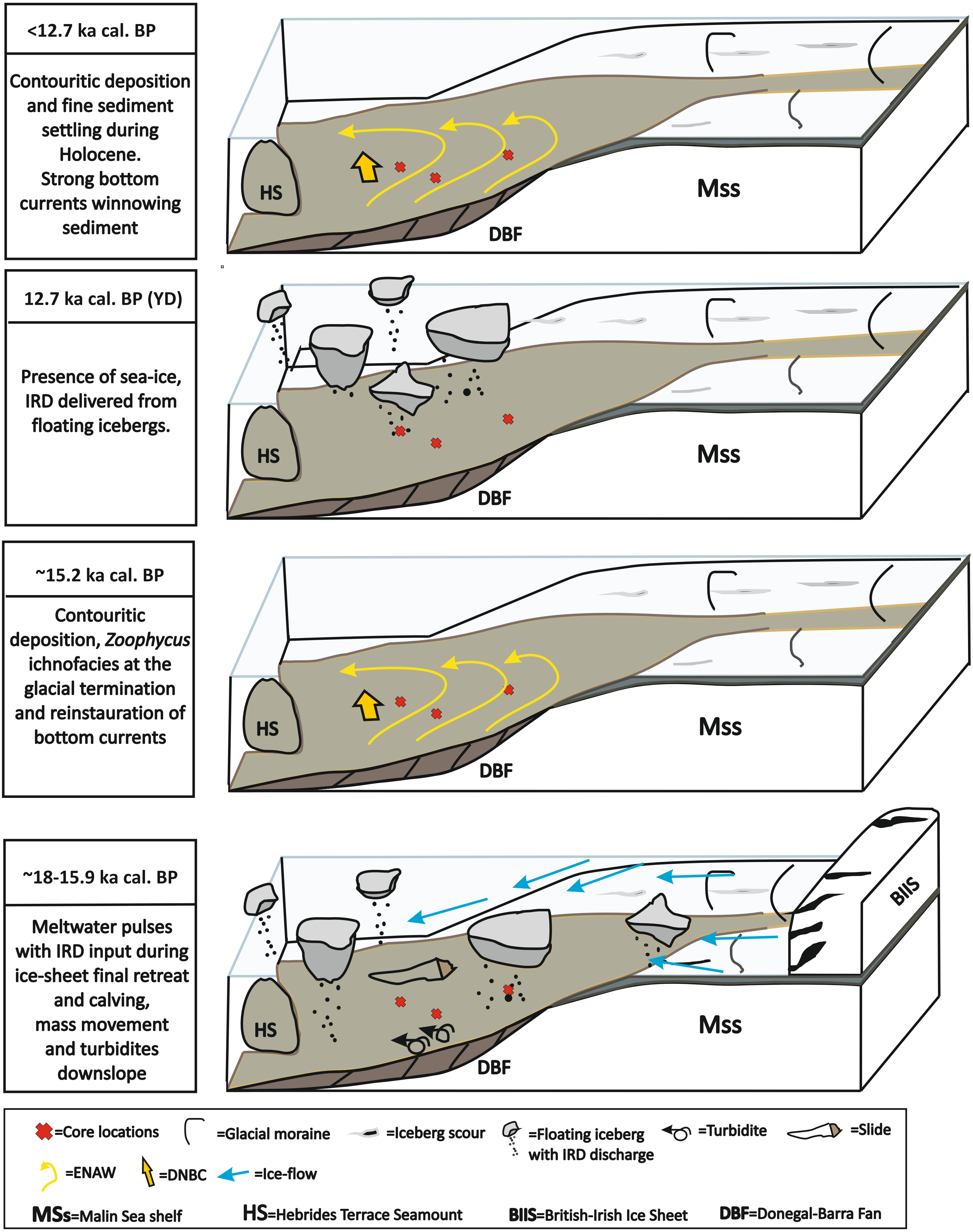

<12.7 ka cal. BP
Contouritic deposition and fine sediment settling during Holocene. Strong bottom currents winnowing sediment
HS
Mss
DBF
12.7 ka cal. BP (YD)
Presence of sea-ice, IRD delivered from floating icebergs.
HS
Mss
DBF
~15.2 ka cal. BP
Contouritic deposition, *Zoophycus* ichnofacies at the glacial termination and reinstauration of bottom currents
HS
Mss
DBF
~18-15.9 ka cal. BP
Meltwater pulses with IRD input during ice-sheet final retreat and calving, mass movement and turbidites downslope
HS
Mss
DBF
BIIS
=Core locations
=Glacial moraine
=Iceberg scour
=Floating iceberg with IRD discharge
=Turbidite
=Slide
=ENAW
=DNBC
=Ice-flow
MSs=Malin Sea shelf
HS=Hebrides Terrace Seamount
BIIS=British-Irish Ice Sheet
DBF=Donegal-Barra Fan